ANALYSIS OF THE ROLE OF MIRNAS IN OVARIAN CANCER METASTASIS

A Dissertation
Presented to
The Academic Faculty

by

Mengnan Zhang

In Partial Fulfillment
of the Requirements for the Degree
Doctor of Philosophy in Bioinformatics in the
School of Biological Sciences

Georgia Institute of Technology
May 2019

ANALYSIS OF THE ROLE OF MIRNAS IN OVARIAN CANCER METASTASIS

Approved by:

Dr. John F. McDonald, Advisor
School of Biological Sciences
Georgia Institute of Technology

Dr. Jung H. Choi
School of Biological Sciences
Georgia Institute of Technology

Dr. I. King Jordan
School of Biological Sciences
Georgia Institute of Technology

Dr. Ronghu Wu
School of Chemistry & Biochemistry
Georgia Institute of Technology

Dr. Fredrik O. Vannberg
School of Biological Sciences
Georgia Institute of Technology

Date Approved: March 26, 2019

To my family

ACKNOWLEDGEMENTS

Firstly, I would like to thank my advisor, Dr. John McDonald, who believed in me and endlessly supported me during my entire PhD study. John guided me to see the fun of scientific research, challenged me to be independent and strong critical thinker, and mentored me to be a "comfortable" public speaker. His kindness, patience, and immense knowledge helped me in all the time of my research. I wouldn't be able to accomplish my achievements without his guidance. I am extremely grateful and proud to be a McDonald lab member.

I also want to express my sincere thanks to my thesis committee members (Dr. King Jordan, Dr. Fredrik Vannberg, Dr. Jung Choi, and Dr. Ronghu Wu) for their great support and invaluable advice. I am thankful to Dr. Jordan for his insightful comments and hard questions, which motivated me to broaden my project. I am grateful to Dr. Vannberg and Dr. Choi, who patiently guided me through the fundamental bioinformatics courses. I am also appreciative of Dr. Wu, an expert in proteomics, who has always been supportive and encouraging of my research. Thank you all for your service on my committee.

My sincere thanks also go to all the McDonald lab members: Dr. L. DeEtte McDonald for her love, care, and support, which make our lab feel like home; Dr. Minati Satpathy, Dr. Lilya Matyunina, Dr. Lijuan Wang, Dr. Yuehua Wang, and Dr. Neda Jabbari for their guidance and constructive comments; Evan Clayton and Dongjo Ban for their help and support on computational analysis; Katie Young and Nick Stone for their suggestions and comments that sharpen my research. Thank you all for your support.

And finally, last but by no means least, I would like to thank my family members for their unconditional love and support. I cannot thank my parents enough for what they've done for me: my mom, who always put me before herself; my dad, who has been my shoulder, friend, and companion. I want to thank my husband for always making my life easier for me.

Thank you all for your encouragement!

TABLE OF CONTENTS

LIST OF TABLES

LIST OF FIGURES

LIST OF SYMBOLS AND ABBREVIATIONS

CDH1	E-cadherin
CTSB	cathepsin B
EMT	Epithelial-Mesenchymal Transition
FBS	fetal bovine serum
FC	fold change
FDR	false discovery rate
FN1	fibronectin
GAPDH	glyceraldehyde-3-Phosphate Dehydrogenase
KRT7	keratin, type II cytoskeletal 7
KRT8	keratin, type II cytoskeletal 8
KRT18	keratin, type I cytoskeletal 18
MAPK	mitogen-activated protein kinase
MET	Mesenchymal-Epithelial Transition
miRNA	MicroRNA
MOC	metastatic ovarian cancer
MYA	million years ago
OC	ovarian cancer
OM	omentum
OV	ovary
PLS1	plastin 1
POC	primary ovarian cancer
qRT-PCR	quantitative real-time polymerase chain reaction

RMA	Robust Multi-Array Average
RPMI	Roswell Park Memorial Institute
siRNA	small interfering RNA
UTR	untranslated region
VEGF	vascular endothelial growth factor
VIM	vimentin
WNT5A	wnt Family Member 5A
ZEB1	zinc finger E-box-binding homeobox 1
ZEB2	zinc finger E-box-binding homeobox 2

SUMMARY

The cancer burden is rising globally, which exerts a severe impact on both the cancer patients and society. Cancer metastasis is the major cause of cancer mortality and accounts for about 90% of cancer deaths. Cancer metastasis develops through a complex multistep process, including dysregulated gene expression changes. These changes are mainly caused by somatic genetic alterations, epigenetic changes, and binding of trans-acting modulators including miRNAs [1, 2]. It is estimated that miRNAs regulate at least 60% of the genes in the human genome [3]. The defects in miRNA expression regulations and target sites are frequently observed in cancer metastasis [4, 5].

miRNAs can affect multiple aspects of cancer metastasis including epithelial to mesenchymal transition (EMT) and mesenchymal to epithelial transition (MET). miR-200 family of miRNAs have been previously implicated to be important in the regulation of EMT/MET in multiple types of cancer [6, 7]. miR-205, a miRNA that is sequentially divergent from miR-200 family, has been shown to induce MET in kidney cancer [8]. Given that even a single nucleotide substitution within the seed region of miRNAs can dramatically change the spectrum of regulated mRNA target genes, it is remarkable that miR-205 can regulate the MET process similarly to the miR-200 family members [9]. To better understand the molecular mechanisms of how sequentially divergent miRNAs could bring about similar morphological changes characteristic of MET, we conducted the studies in Chapter 2. We present evidence that miR-205 and the miR-200 family of miRNAs coordinately induce MET in mesenchymal-like ovarian cancer cells by affecting both direct and indirect changes in the expression of genes. We demonstrate that the

majority of changes in gene expression commonly induced by ectopic over-expression of the sequentially divergent miRNAs are the result of indirect regulatory controls, specifically in the changes in expression of EMT/MET-associated genes. Collectively, our findings suggest that the regulation of EMT/MET associated genes by miR-205 is the result of convergent evolution facilitated by the relatively recent clustering of miR-205 with members of the miR-200 family on human chromosome 1 approximately 80 MYA.

Like gene expression regulation, miRNA-mediated regulation is often cancer/cell-type specific. To better understand the molecular mechanisms underlying this specificity, we examined the molecular and phenotypic responses of three mesenchymal-like cancer cell lines (two ovarian/one prostate) to ectopic over-expression of three sequentially divergent miRNAs previously implicated in the EMT/MET processes. In Chapter 3, we demonstrate the variability of the sequentially divergent miRNAs in inducing MET in ovarian and prostate cancer cells. We report that the ability of these sequentially divergent miRNAs to induce MET in these cells is found to be associated with inherent differences in the starting molecular profiles of the untreated cancer cells, as well as, variability in trans-regulatory controls modulating the expression of genes targeted by the individual miRNAs. Our results help support the view that miRNAs have significant potential as cancer therapeutic agents.

miRNAs can regulate their target gene expression through different mechanisms, including mRNA degradation and/or translational inhibition [10]. As a result, the miRNA targets can be translationally repressed with or without a corresponding decrease in mRNA abundance, or the miRNA targets can degrade mRNAs with or without a corresponding protein reduction. In order to understand these mRNA and protein non-correlated changes

and contributions of miRNAs during ovarian cancer development, we integrated global miRNA and mRNA expression microarray data with proteomics data of the discrete tumor samples collected from the ovary and from the omentum of the same ovarian cancer patient. In Chapter 4, we present the miRNA mediated non-correlated changes between mRNA and protein levels. Our results prove that the overall correlation between changes in levels of mRNA and protein is low (r=0.38) and the majority of changes are on the protein level with no corresponding changes on their mRNA level. We provide computational and experimental evidence that a significant fraction of changes between mRNA and protein levels are mediated by miRNAs. Our findings provide an example of the contribution of miRNAs to the regulatory coordination of changes on the mRNA and protein levels to the metastatic process.

CHAPTER 1. INTRODUCTION

Cancer is a leading cause of death worldwide. According to the latest global data, the cancer burden is estimated to have risen to 18.1 million new cases and 9.6 million deaths in 2018. Most cancer deaths are caused by cancer metastasis, not the primary tumor. It is estimated that metastasis is responsible for about 90% of cancer deaths [11].

Metastasis occurs through a multi-step process known as the invasion-metastasis cascade that includes the dissemination of cancer cells from primary tumors and the subsequent seeding of new tumor colonies in distant organs [12-14]. The dissemination enables malignant tumor cells to acquire certain traits that allow them to leave the primary site and travel through the lymphatic and hematogenous vessels to the distant metastatic site. The biological process that gives rise to these steps is termed "epithelial-mesenchymal transition" (EMT). During EMT, cancer cells lose their epithelial properties and gain mesenchymal features [12, 14]. The EMT process modifies the adhesion molecules expressed by the cell, induces growth arrest, and increases resistance to apoptosis, allowing the cells to adopt a migratory and invasive behavior [15-17]. In order to allow growth once cancer cells arrive at the distant metastatic site, the cancer cells undergo mesenchymal-to-epithelial transition (MET) to regain a proliferative state and facilitate the formation of metastatic tumors at distant organs [18]. EMT and MET form the initiation and completion of the invasion-metastasis cascade [19].

Metastasis can be regulated by a complex network of interconnected signaling pathways, transcription factors, and post-transcriptional factors [20]. Signaling pathways include transforming growth factor-β (TGF-β), epidermal growth factor (EGF), insulin-

like growth factor (IGF), fibroblast growth factor (FGF), vascular endothelial growth factor (VEGF), WNT, and NOTCH pathway [21-25]. These pathways ultimately stimulate transcriptional factors, such as zinc finger E-Box binding homeobox (ZEB1 and ZEB2), snail family transcriptional repressor (SNAI1 and SNAI2), and twist helix-loop-helix transcription factor (TWIST1 and TWIST2) [26-28]. Eventually, these transcription factors dynamically regulate the expression of biomarker genes of metastasis, such as E-cadherin and N-cadherin, which facilitates the metastasis process. In addition to transcriptional level regulation, metastasis can also be regulated on a post-transcriptional level through regulatory RNAs, including microRNAs [29, 30].

MicroRNAs (miRNAs) are small (22-25 nucleotides long) noncoding RNA molecules that have been shown to be the important post-transcriptional regulators of gene expression [31]. To date, over 2,500 potential human miRNAs have been recorded in miRBase v22 and their number is increasing rapidly [32]. miRNAs are typically transcribed by RNA polymerase II (Pol II) in the nucleus to generate the large primary transcripts (pri-miRNA). The initial processing of the primary transcripts is mediated by Drosha-DiGeorge syndrome critical region gene 8 (*DGCR8*) complex that generates a pre-miRNA that is about 70 nucleotides in length. This pre-miRNA transcript is transported into the cytoplasm by the nuclear export factor, exportin 5, and further processed by the cytoplasmic RNase III Dicer to form the miRNA duplexes. Dicer, TAR RNA-binding protein (TRBP), and Argonaute (AGO) mediate the processing of miRNA duplexes and the assembling of the RNA-induced silencing complex (RISC) [33]. Within this complex, one strand of the miRNA duplex is removed, resulting in a single stranded miRNA. RISC guides the miRNA to bind to target complementary regions (typically 3'-UTR region) of

mRNA transcripts through base pairing. miRNA target recognition is primarily determined by pairing of the highly conserved miRNA seed sequence (nucleotides 2-8 of the miRNA) to complementary sites in target mRNAs [34, 35]. Depending on the complementation between the miRNA and target mRNA sequences, miRNAs can generally regulate the gene expression of the mRNA transcript in two ways. When there is a near-perfect complementary match between the miRNA and target mRNA sequence, miRNA degrades the target mRNA transcript. When there is a partial complementary match between the miRNA and the target mRNA sequence, the miRNA inhibits the target mRNA translation [36].

Many miRNAs have been shown to be involved in metastasis, including the miR-200 family of miRNAs. miR-200 family members have been reported to facilitate cancer metastasis by inducing MET in multiple types of cancer [37, 38]. The miR-200 family of miRNAs contains five miRNAs that can be separated into two functional groups based on their seed sequences. Functional group I consists of miR-200b, miR-200c, and miR-429. Functional group II consists of miR-141 and miR-200a. The seed sequences of these two functional groups only differ by one nucleotide: AAUACUG for group I and AACACUG for group II. Even though there are variations in molecular response and chemotherapy drug sensitivity between the two functional groups of miR-200 family members, all five members of miR-200 family are able to induce MET in ovarian cancer [7].

Given that even a single nucleotide substitution within the highly conserved seed region of miRNAs can dramatically change the spectrum of regulated mRNA target genes [9], it is remarkable that families of miRNAs sequentially divergent from one another can similarly regulate the EMT/MET process in a diversity of cancer cells. For example, miR-

205, although sequentially highly divergent from members of the miR-200 family, has been reported to display a similar ability to induce MET in mesenchymal-like lung [39] and prostate [40] cancer cells. To better understand the molecular mechanisms of how sequentially divergent miRNAs could bring about similar morphological changes characteristic of MET, we conducted the studies in Chapter 2. We present evidence that helps explain how sequentially divergent miRNAs (miR-205 and miR-200 family members) are able to induce MET in ovarian cancer HEY cells. We first demonstrate that miR-205 and the miR-200 family of miRNAs both induce MET in mesenchymal-like ovarian cancer cells by affecting both direct and indirect changes in the expression of genes. We next demonstrate that the majority of changes in gene expression commonly induced by ectopic over-expression of the miR-200 family of miRNAs and miR-205 are the result of indirect regulatory controls, specifically in the changes in expression of EMT/MET-associated genes. While only two direct targets of these miRNAs (ZEB1 and WNT5A) are commonly down regulated in response to over expression of miR-205 and/or the miR-200 family of miRNAs, down regulation of these genes alone or in combination only partially recapitulated the changes induced by the miRNAs. This indicates an auxiliary contribution of other direct and/or indirect regulatory changes induced in common or individually by the miRNAs. We go on to provide evidence that regulation of EMT/MET associated genes by miR-205 is the result of convergent evolution brought about by a translocation event linking miR-205 with members of the miR-200 family on human chromosome 1 approximately 80 MYA.

Individual miRNAs can target hundreds or thousands of mRNAs based on sequence complementarity, but a substantial fraction of these predicted interactions may depend on

specific cellular context. Recent studies have demonstrated that the overexpression of specific miRNAs has the ability to induce MET in a variety of cancer cells [41-44]. Interestingly, the ability of individual miRNAs to induce MET when over-expressed in cancer cells is often cancer/cell-type specific. To better understand the molecular processes underlying this specificity, we examined the molecular and phenotypic responses of three mesenchymal-like cancer cell lines (two ovarian/one prostate) to ectopic over-expression of three sequentially divergent miRNAs (miR-203a, miR-205, and miR-429) previously implicated in the EMT/MET processes [45, 46]. In Chapter 3, we demonstrate that the overexpression of miR-205 induces a morphological change to a more rounded/cuboidal phenotype consistent with MET in the two OC cells (HEY and SKOV3) but not in prostate cancer cells (PC3) relative to negative controls. In contrast, miR-203a induces morphological changes characteristic of MET in PC3 cells but not in the HEY and SKOV3 cells while miR-429 induces morphological changes characteristics of MET in all three of the cell lines. We report that the ability of these sequentially divergent miRNAs to induce MET in these cells is found to be associated with inherent differences in the starting molecular profiles of the untreated cancer cells, as well as, variability in trans-regulatory controls modulating the expression of genes targeted by the individual miRNAs. Our results help support the view that miRNAs have significant potential as cancer therapeutic agents.

The central dogma of biology defines the flow of genetic information within a biological system, as “DNA makes RNA and RNA makes protein” [47]. The nucleotide sequence of a gene determines the sequence of its mRNA product and the mRNA sequence determines the amino acid sequence of the resulting protein. As mRNA is ultimately

translated into protein, it is often assumed that changes on the mRNA level are correlated with changes on the protein level; however, the correlation between mRNA and protein abundances in the cell has been reported to be notoriously poor [48]. Systematic studies quantifying transcripts and proteins at genomic scales revealed the importance of multiple processes beyond transcript concentration that contribute to establishing the expression level of a protein, including protein synthesis delay, protein half-life, and translation rate modulation through the binding of non-coding RNAs including miRNAs [49-51]. miRNAs can regulate its target gene expression through different mechanisms, including mRNA degradation and/or translational inhibition [52]. As a result, the miRNA targets can be translationally repressed with or without a corresponding decrease in mRNA abundance, or the miRNA targets degrade mRNA with or without a corresponding protein reduction.

Over the last two decades, high-throughput technologies have been developed to support the large-scale quantitative analysis of transcriptomes and proteomes, which enables the systematic comparison of the mRNA and protein changes in parallel. In order to understand the mRNA and protein non-correlated changes and contributions of miRNAs during ovarian cancer development, we integrated global miRNA and mRNA expression microarray data with proteomics data of the discrete tumor samples collected from the ovary and from the omentum of the same ovarian cancer patient. In Chapter 4, we present evidence that the majority of changes in gene expression between tumor samples collected from the ovary and omentum of the same patient occur at the post-transcriptional level. We first proved that the overall correlation between global changes in levels of mRNAs and their encoding proteins is low (r=0.38). We next verified that the majority of differences are on the protein level with no corresponding change on the mRNA level. More

importantly, we revealed the limitation of making functional predictions from the differentially expressed genes from RNA profiling alone. We further validated that a significant fraction of the discordance in changes on the RNA and protein levels between our samples are mediated by miRNAs. Our results provide an example of the contribution of miRNAs in the regulatory coordination of changes on the RNA and protein levels to enhance metastasis.

CHAPTER 2. SEQUENTIALLY DIVERGENT MIRNAS CONVERGE TO INDUCE MESENCHYMAL-TO-EPITHELIAL TRANSITION IN OVARIAN CANCER CELLS THROUGH DIRECT AND INDIRECT REGULATORY CONTROLS

2.1 Abstract

Background: Epithelial-to-mesenchymal transition (EMT) has been shown to be similarly regulated by multiple miRNAs, some displaying little or no sequence identity. While alternate models have been proposed to explain the functional convergence of sequentially divergent miRNAs, little experimental evidence exists to elucidate the underlying mechanisms involved.

Methods: Representative members of the miR-200 family of miRNAs and the sequentially divergent miR-205 miRNA were independently overexpressed in mesenchymal-like ovarian cancer (OC) cells resulting in mesenchymal-to-epithelial transition (MET). Gene expression analyses combined with target gene prediction and siRNA knockout experiments identified genes directly or indirectly regulated by each miRNA.

Results: The sequentially divergent miR-205 and the miR-200 family of miRNAs coordinately induce MET in mesenchymal-like OC cells by affecting both direct and indirect changes in the expression of genes previously associated with EMT/MET. Only two direct targets of these miRNAs (*ZEB* 1 and *WNT5A*) are commonly down-regulated in response to over-expression of miR-205 and/or the miR-200 family of miRNAs. Down-

regulation of these genes, alone or in combination, only partially recapitulates the changes induced by the miRNAs indicating an auxiliary contribution of direct and/or indirect changes regulated by the miRNAs. Combined gene expression analyses and phylogenetic comparisons support an evolutionarily more recent involvement of miR-205 in the EMT/MET process.

Conclusions: MiR-205 and the miR-200 family of miRNAs coordinately induce MET in mesenchymal-like OC cells by inducing both direct and indirect regulatory changes in the expression of EMT/MET associated genes. Regulation of EMT/MET associated genes by the sequentially divergent miR-205 is the likely result of convergent evolution facilitated by chromosomal clustering of miR-205 with members of the miR-200 family ~ 80 MYA.

2.2 Introduction

Epithelial-to-mesenchymal transition (EMT) and mesenchymal-to-epithelial transition (MET) are reciprocal molecular processes essential in early embryonic development that have been co-opted by cancer cells to facilitate tumor metastasis [53]. Recent studies have demonstrated that both EMT and MET can be induced by modulations in cellular levels of microRNAs (miRNAs), a well-studied class of small regulatory RNAs [54]. Our laboratory has been particularly interested in the ability of members of the sequentially homologous miR-200 family of miRNAs to induce MET when ectopically overexpressed in mesenchymal-like ovarian cancer (OC) cells [7]. Given that even a single nucleotide substitution within the highly conserved seed region of miRNAs can dramatically change

the spectrum of regulated mRNA target genes [9], it is remarkable that families of miRNAs sequentially divergent from one another can similarly regulate the EMT/MET process in a diversity of cancer cells. For example, miR-205, although sequentially highly divergent from members of the miR-200 family, has been reported to display a similar ability to induce MET in mesenchymal-like lung [39] and prostate [40] cancer cells. We report here that although miR-205 has little to no sequence homology with members of the miR-200 family of miRNAs, it induces morphological transitions in mesenchymal OC cells that are morphologically indistinguishable from those induced by members of the sequentially divergent miR-200 family. We show that miR-205 and the miR-200 family of miRNAs coordinately induce MET in mesenchymal-like OC cells by affecting both direct and indirect changes in the expression of genes previously associated with EMT/MET. While two direct targets of these miRNAs (*ZEB* 1 and *WNT5A*) are commonly down-regulated in response to over-expression of miR-205 and/or the miR-200 family of miRNAs, down-regulation of these genes alone or in combination only partially recapitulates the changes induced by the miRNAs indicating an auxiliary contribution of other direct and/or indirect regulatory changes induced in common or individually by the miRNAs. Finally, evidence is presented indicating that regulation of EMT/MET associated genes in humans by miR-205 is the result of convergent evolution facilitated by the clustering of miR-205 with members of the miR-200 family on chromosome 1 ~80 MYA [55].

2.3 Materials and Methods

2.3.1 Cell culture and transfection

The HEY cell line was kindly provided by Gordon Mills, Department of Molecular Therapeutics, University of Texas, MD Anderson Cancer Center. Cells were cultured in RPMI 1640 (Mediatech, Manassas, VA) supplemented with 10% FBS (Fetal Bovine Serum; Atlanta Biologicals, Lawrenceville, GA) and 1% antibiotic-antimycotic solution (Mediatech-Cellgro). 1×10^5 cells were seeded per well in 6-well plates. For miRNA transfection, cells at exponential phase of growth were transfected with 33 nM Pre-miR miRNA Precursors (Life Technologies, Carlsbad, CA) using Lipofectamine 2000 (Life Technologies). Pre-miR miRNA Precursor Negative was used as negative control. For siRNA transfection, cells at exponential phase of growth were transfected with 33 nM Silencer Select (Life Technologies) using Lipofectamine 2000 (Life Technologies). Silencer Select Negative Control siRNA was used as a negative control. Cells were allowed to grow for 48 h before RNA extraction.

2.3.2 Microarray analysis

Cells were harvested at 48 h after transfection and RNA extracted and subjected to microarray analysis (Affymetrix, U133 Plus 2; Santa Clara, CA) as previously described [56]. Robust Microarray Averaging (RMA) was used for normalization of microarray signal and summarization using the Affymetrix Expression Console Software (Version 1.4). Statistical analysis of the expression data was carried out using the limma package [57] executed in R. Differentially expressed mRNAs were identified through fold change and FDR adjusted p-value calculated using moderated t-test.

2.3.3 Gene set similarity measurement

The cosine similarity index was used to determine the similarity between two sets of genes [58].

2.3.4 miRNA target prediction

Prediction algorithms were downloaded and implemented (miRanda [59] - (www.microrna.org), miRDB [60] - (http://mirdb.org/download.html), and TargetScan [61] - (http://www.targetscan.org/vert_72/) according to the recommended procedures.

2.3.5 Image analysis

Morphological changes were monitored using an Olympus IX51 microscope (Olympus Optical, Melville, NY) and quantified using CellProfiler cell-imaging software (2.1.0) [62].

2.3.6 Real-time PCR

Total RNA was extracted from cells using the RNeasy Mini Kit (RNeasy, Qiagen, Germantown, MD). Four micrograms of RNA were reversed transcribed into cDNA using the Superscript III First-Strand Synthesis System (Life Technologies) according to the manufacturer's instructions. Real-time PCR was performed using TaqMan Real-Time PCR Master Mixes (Life Technologies) on a CFX96 Real-Time System (Bio-Rad, Hercules,

CA). Expression values were normalized using *GAPDH* as a reference gene. Normalization and fold-change were calculated using the ΔΔCt method.

2.3.7 Western Blot

The total protein concentration of the supernatant was determined using a protein assay reagent kit (Bio-Rad). To the lysates, equal volumes of 2X Laemmli sample buffer were added and the samples were heated to 90 °C for 5 minutes. Equal amounts of proteins were separated by 4–20% gradient precast TGX gel (Bio-Rad) and transferred to nitrocellulose membranes (Bio-Rad). Membranes were blocked with 5% nonfat dry milk in 10 mM Tris buffered saline. After blocking, the membranes were probed with the primary antibody overnight at 4 °C with gentle shaking. Antibodies used are against Zinc Finger E-Box Binding Homeobox 1 (ZEB1 antibody, Cat # 3396, Cell Signaling Technology, Danvers, MA), Wnt Family Member 5A (WNT5A antibody, Cat # 2392, Cell Signaling Technology), and Beta-actin (ACTB antibody Cat # 5441, Sigma, St. Louis, MO). After incubation with the corresponding anti-mouse- or anti-rabbit-horseradish peroxidase-conjugated secondary antibodies (Santa Cruz Biotechnology, Inc., Dallas, TX), the Western blots for specific proteins were detected using an enhanced chemiluminescence (ECL) kit (Life Technologies) and images were developed by Amersham Imager 600 (GE Healthcare, Chicago, IL) according to the manufacturer's instructions.

2.4 Results

2.4.1 miR-205 overexpression induces morphological changes characteristic of MET indistinguishable from those induced by the sequentially divergent miR-200 family of miRNAs.

We have previously reported that ectopic overexpression of miR-200 family members in mesenchymal-like OC cells results in the induction of morphological and molecular changes characteristic of MET [41, 63, 64]. We were interested in determining if ectopic overexpression of miR-205 could induce similar changes despite being sequentially highly divergent from miR-200 family members (Figure 2.1 B). Towards this end, we conducted a series of experiments where two representative members of the miR-200 family (miR-141 and miR-200b) and miR-205 were individually ectopically over-expressed in HEY cells. The results presented in Figure 2.1 A demonstrate that over expression of miR-205 in HEY cells does induce changes in OC HEY cells characteristic of MET that are visually indistinguishable from those induced by the two representative members of the miR-200 family. Cell eccentricity analyses confirm that there is no statistically significant difference between the morphological changes induced by over expression of miR-205 and the two representative members of miR-200 family (Figure 2.1 C). Coordinated increases in the expression of representative epithelial biomarkers (KRT7, KRT8, KRT18) and decreases in the expression of mesenchymal biomarkers (VIM, FN1, ZEB1, ZEB2) are consistent with mesenchymal-to-epithelial transitions in response to over expression of each of the miRNAs (Figure 2.1 D).

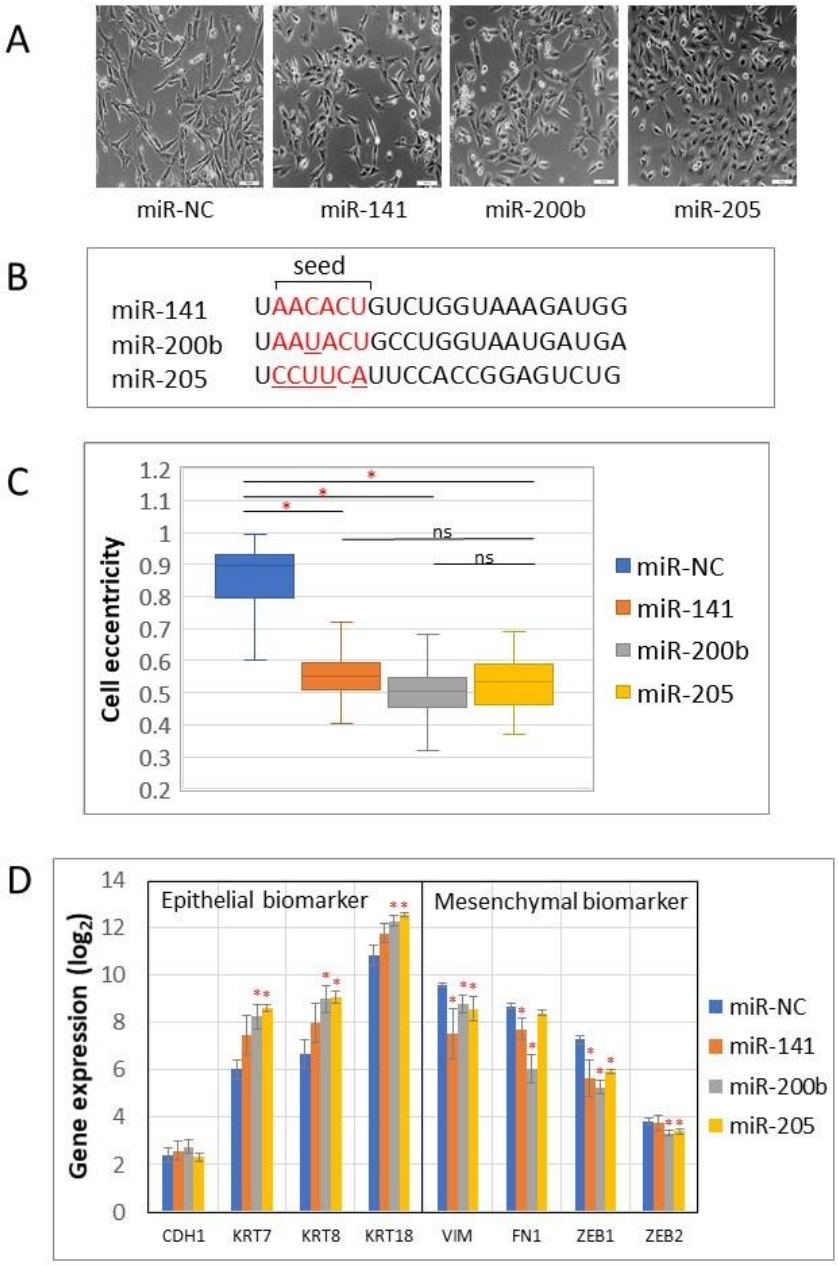

Figure 2.1. miR-205 overexpression induces morphological changes characteristic of MET indistinguishable from those induced by the sequentially divergent miR-200 family of miRNAs. (A) Representative microscopic images of HEY cells 48 h post transfection with miRNAs. (Scale bars, 100 µm). (B) Sequence alignments of miR-141, miR-200b, and miR-205. Seed regions are colored in red. Differences in seed region of miRNAs relative to miR-200b are underlined. (C) The accumulation of rounded epithelial-like cells occurred in miR-141/200b/205 transfected cells 48 h post transfection. (cell eccentricity: a score of 0 = circular shape, a score of 1 = linear

shape; asterisk = p-value < 0.05). Significance of differences is evaluated using Student's t-test. (D) Gene expression of representative epithelial and mesenchymal biomarkers post 48 h transfection with miRNAs evaluated by microarray profiling analyses (compared to miR-NC, p-value < 0.05).

2.4.2 The majority of changes in gene expression commonly induced by ectopic over-expression of the miR-200 family miRNAs and miR-205 are the result of indirect regulatory controls.

In an effort to better understand the molecular changes mediated by over expression of miR-200 family (miR-141 and miR-200b) and miR-205 miRNAs relative to controls, we conducted microarray gene expression analyses (Affymetrix, U133 Plus 2.0 Array; Table A.1) as previously described [65]. We focused initially on changes in gene (mRNA) expression induced in common by ectopic over-expression of the two representative members of the miR-200 family. Of the 6416 genes significantly differentially expressed in response to ectopic over-expression of the miR-200 family members, 1994 genes were induced in common (Figure 2.2 A). The cosine similarity index of differentially expressed genes between the miR-200 family members is 0.51. This value of similarity was increased when comparing differentially expressed genes between miR-205 and miR-141/miR-200b. 3453 genes were induced in common between miR-205 and miR-141, with a similarity index of 0.65 (Figure 2.2 B), while 2197 genes were induced in common between miR-205 and miR-200b, with a similarity index of 0.59 (Figure 2.2 C). Overall, 91.3% (1821/1994) of the genes differentially expressed by ectopic over-expression of both miR-200 family miRNAs were also significantly differentially expressed in response to over expression of miR-205 (Figure 2.2 D).

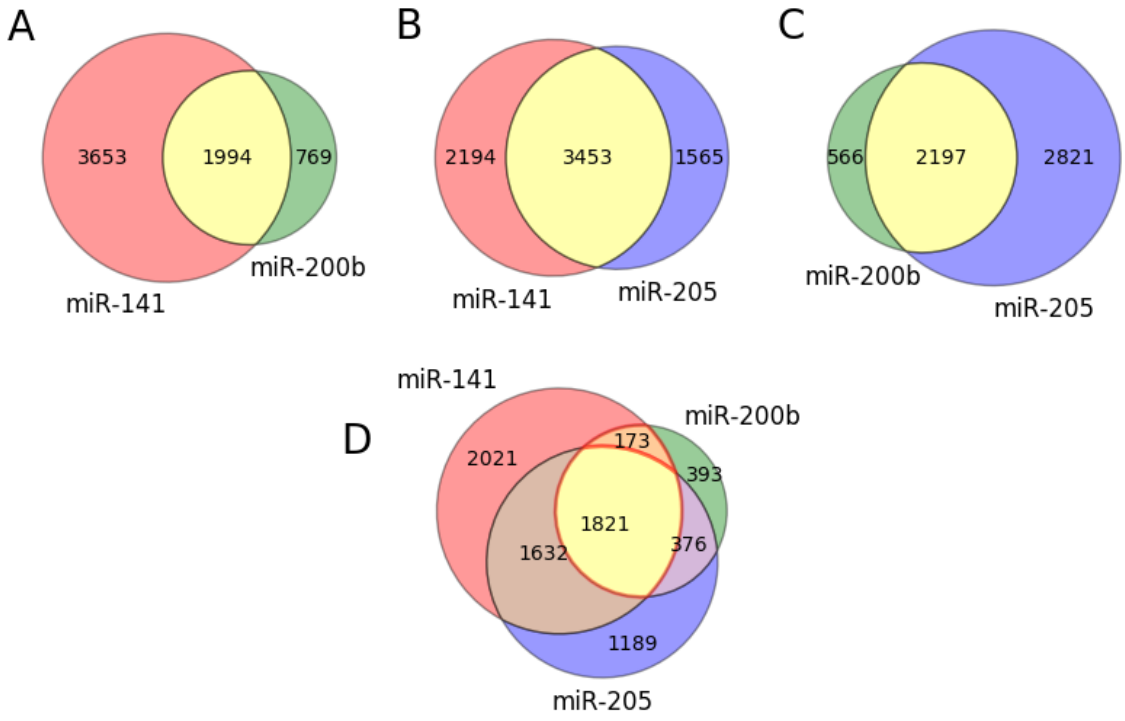

Figure 2.2. Analysis of differentially expressed genes after transfection of miR-200 family members (miR-141 and miR-200b) and miR-205. (A) Venn diagram showing the intersection of differentially expressed genes between miR-141 and miR-200b. (B) Venn diagram showing the intersection of differentially expressed genes between miR-141 and miR-205. (C) Venn diagram showing the intersection of differentially expressed genes between miR-200b and miR-205. (D) Venn diagram showing the intersection of differentially expressed genes between miR-141, miR-200b, and miR-205. Differentially expressed genes between categories were filtered (FDR < 0.05 and fold change > 1.5).

The fact that the miR-200 family and miR-205 miRNAs are sequentially highly divergent makes it unlikely that they directly target a high proportion of the same genes. We confirmed this by employing three independent prediction algorithms (miRanda [59], miRDB [60], TargetScan [61]) to identify direct target genes of the three miRNAs analyzed in this study (Table A.2, Table A.3, Table A.4). For example, according to the miRanda miRNA target prediction algorithm [59], 3943, 4027, and 2941 genes are predicted to be

direct target genes of miR-141, miR-200b, and miR-205, respectively. Among these, 1440 genes are predicted to be direct target genes of both miR-141 and miR-200b, but only 444 out of these 1440 genes (30.8%) are predicted to be direct target genes of miR-205 (Figure 2.3).

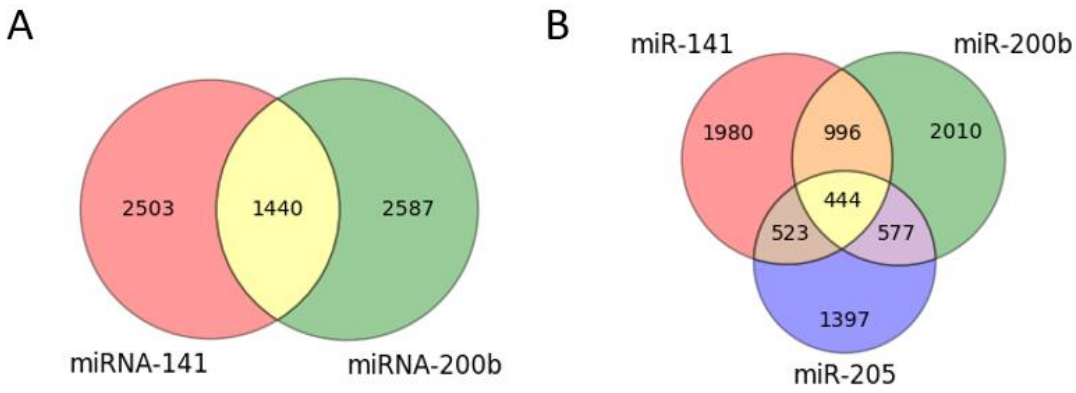

Figure 2.3. Analysis of intersection between miRanda-predicted direct target genes of miR-200 family members (miR-141 and miR-200b) and miR-205. (A) Venn diagram showing the intersection of direct target genes between miR-141 and miR-200b. (B) Venn diagram showing the intersection of direct target genes between miR-141, miR-200b, and miR-205.

Overall, our gene expression analysis, demonstrates that of the 1994 genes displaying a significant change in expression in response to overexpression of the miR-200 family miRNAs, only 181 genes (9.1%) are predicted to be direct target genes of both of these miRNAs (Figure 2.4 A). Of the 1821 genes induced in common by the miR-200 family miRNAs and miR-205, only 61 (3.3%) are predicted to be direct target genes of all of these miRNAs (Figure 2.4 B). These results indicate that the vast majority of the changes

in gene expression commonly induced by ectopic over-expression of the miR-200 family miRNAs and miR-205 are the result of indirect regulatory effects.

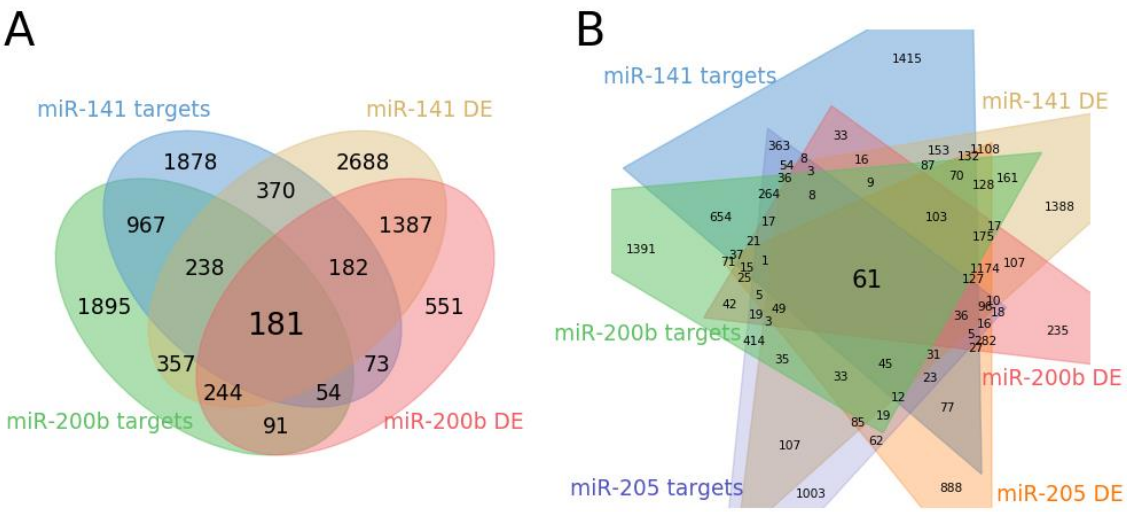

Figure 2.4. Analysis of the intersection between differentially expressed genes and miRNA target genes after transfection of miR-200 family members (miR-141 and miR-200b) and miR-205. (A) Venn diagram showing the intersection of differentially expressed genes and miRanda-predicted miRNA target genes between miR-141 and miR-200b. (B) Venn diagram showing the intersection of differentially expressed genes and miRanda-predicted miRNA target genes between miR-200 family members (miR-141 and miR-200b) and miR-205. Differentially expressed genes between categories were filtered (FDR < 0.05 and fold change > 1.5).

2.4.3 The majority of changes in expression of EMT/MET-associated genes commonly induced by ectopic overexpression of the miR-200 family miRNAs and miR-205 are also the result of indirect regulatory controls.

We were next interested in determining if similar trends apply to a subset of genes previously identified as being directly involved in EMT/MET. For these studies, we focused our analysis on 84 genes that have been previously linked to the EMT/MET

process [66]. Thirty-eight of these 84 genes were significantly differentially expressed by ectopic overexpression of at least one of the miR-200 family members (miR-141 and miR-200b) or miR-205 (Figure 2.5). Of these 38 genes, 17 (44.7%) were commonly induced by both members of the miR-200 family tested. Interestingly, 15 out of these 17 genes (88.2%) are also differentially expressed when miR-205 is included in the analysis. Of the 17 EMT/MET genes induced in common by the miR-200 family members, only four (23.5%) are predicted to be direct target genes of these miRNAs. Likewise, of the 15 EMT genes induced in common by the miR-200 family and miR-205 miRNAs, only two (13.3%) genes (*ZEB1 and WNT5A*) are predicted to be directly targeted in common by these miRNAs (Figure 2.5).

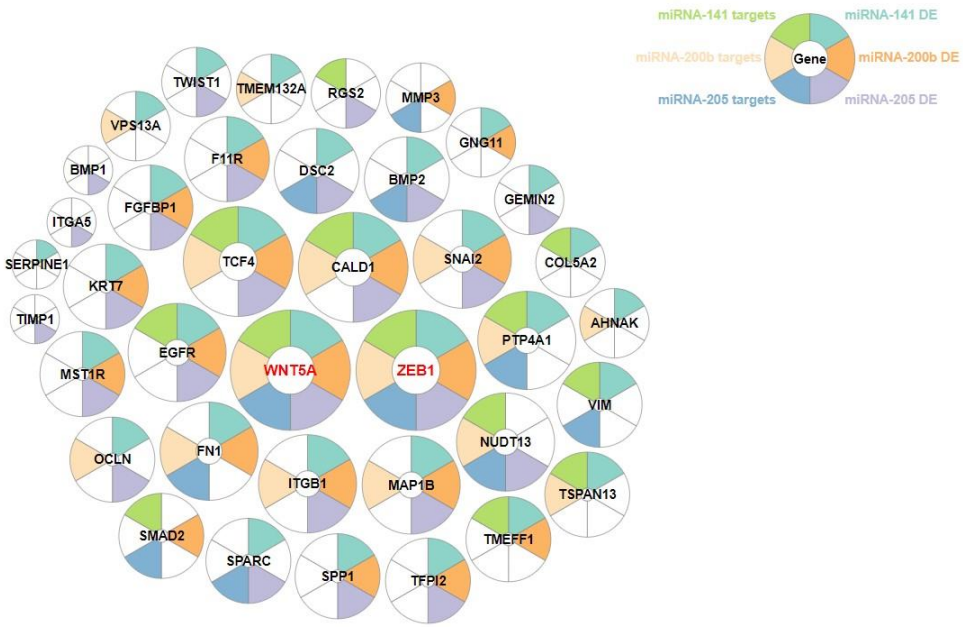

Figure 2.5. Analysis of the intersection between differentially expressed EMT/MET genes and miRNA target genes after transfection of miR-200 family members (miR-141 and miR-200b) and miR-205. Thirty-eight EMT/MET genes were significantly differentially expressed by ectopic over-expression of at least one of the miR-200 family members (miR-141 and miR-200b) or miR-205. Each circle represents a gene. The right half of the circle represents if the gene has been differentially expressed

(DE) after transfection of miR-141 (right-top), miR-200b (right-middle), or miR-205 (right-bottom) in HEY cells after 48 h transfection. The left half of the circle represents if the gene is a direct target gene of miR-141 (left-top), miR-200b (left-middle), or miR-205 (left-bottom). The white slice of the circle means either this gene is not differentially expressed after transfection, or this gene is not the direct target of the corresponding miRNA. The non-white slice of the circle means either this gene is differentially expressed after transfection, or this gene is the direct target of the corresponding miRNA. Genes highlighted in red are the EMT/MET genes that are differentially expressed direct target genes of both miR-200 family members (miR-141 and miR-200b) and miR-205.

2.4.4 Knockdown of ZEB1 and/or WNT5A induces intermediate morphological changes in HEY cells

Of the EMT-associated genes directly targeted in common by miR-141, miR-200b and miR-205, only *ZEB1* and *WNT5A* were consistently down regulated after ectopic overexpression of these miRNAs (Figure 2.6 A). This raises the possibility that reduced expression of these genes may alone be responsible for the morphological changes associated with over expression of the miRNAs. To test this hypothesis, we ectopically over-expressed siRNAs against ZEB1 and WNT5A (alone and in combination) in HEY cells. While knockdown of ZEB1 and WNT5A, alone or in combination, resulted in a significant decrease in the expression of these genes on both the mRNA (Figure 2.6 B) and protein levels (Figure 2.6 C), the cell eccentricity analyses indicated a non-significant overall difference in cell morphology from the negative controls (Figure 2.7 A, B). However, detailed examination of cell images in the ZEB1/WNT5A knockdown groups reveals that some cells clearly exhibit a cuboidal, epithelial-like phenotype after treatment indicative of a partial or intermediate induction of MET (*e.g.*, note cells circled in yellow in Figure 2.7 A).

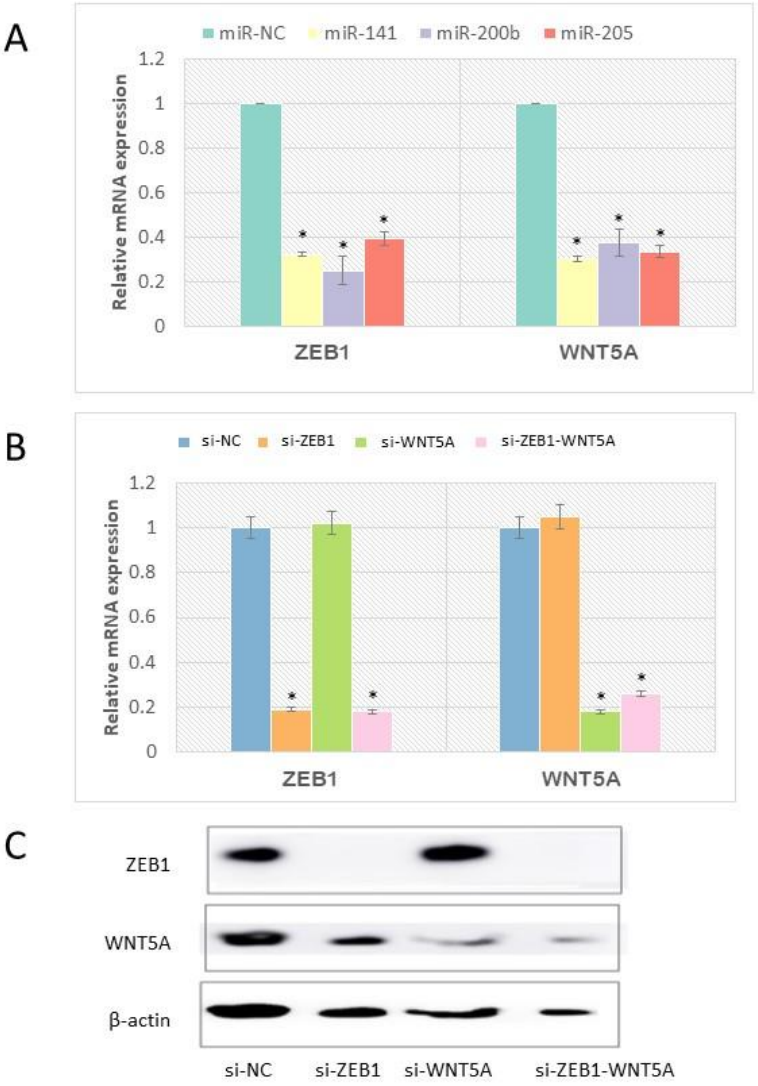

Figure 2.6. Analysis of ZEB1 and WNT5A expression in miRNA and siRNA transfected cells. (A) ZEB1 and WNT5A expression were consistently down regulated after transfection of the miRNAs. Asterisks represent statistically significant differences from the negative control group. (*p-value < 0.05) (B) Relative mRNA expression of ZEB1 and WNT5A as determined by qRT-PCR shows a significant decrease on the mRNA levels in the corresponding individual transfections and combined transfection groups. Asterisks represent statistically significant differences from the negative control group. (*p-value < 0.05) (C) Western blot analysis of ZEB1 and WNT5A proteins both display reduced levels of protein in the corresponding individual transfections and combined transfection groups.

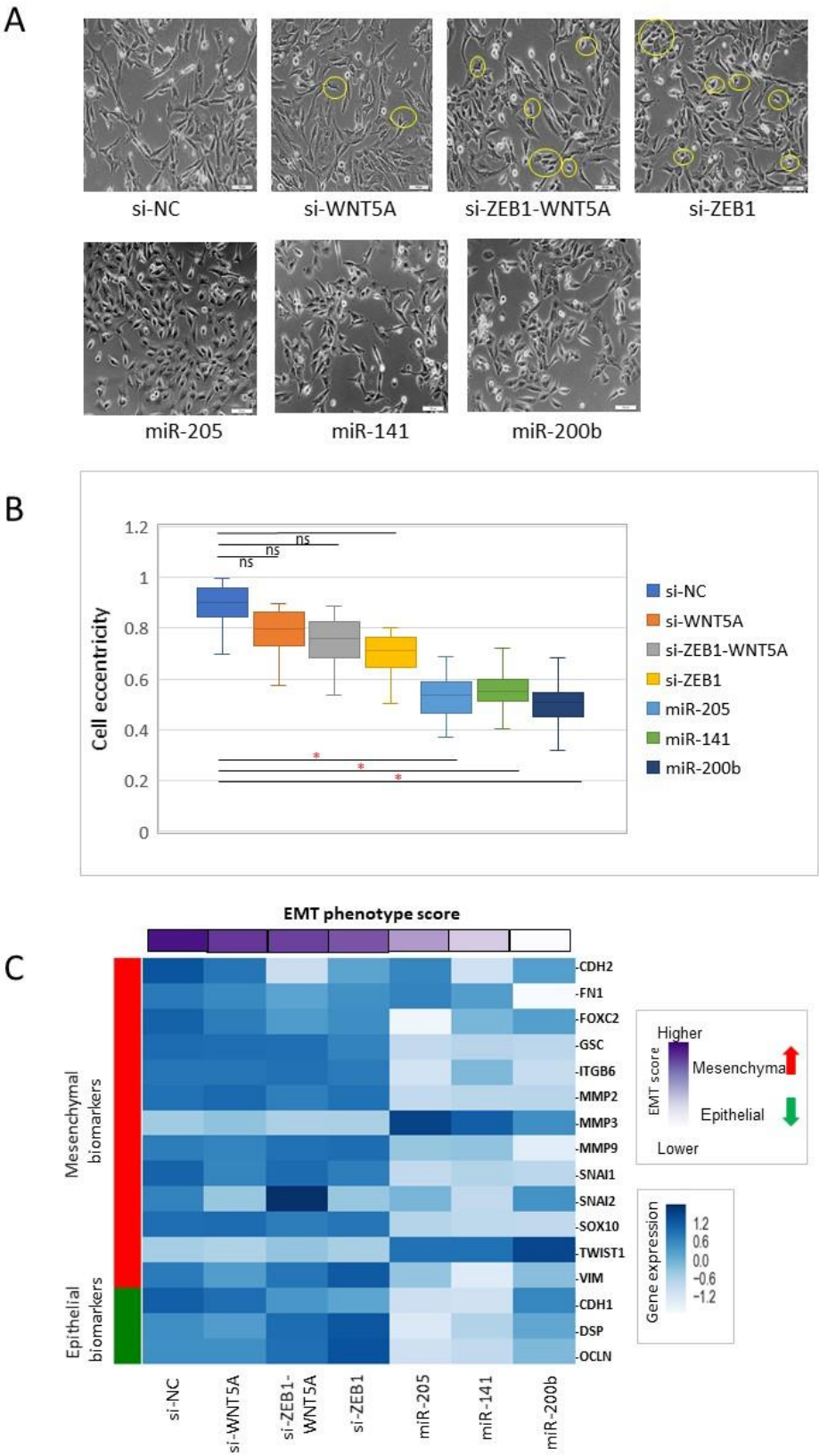
A
si-NC
si-WNT5A
si-ZEB1-WNT5A
si-ZEB1
miR-205
miR-141
miR-200b
B
Cell eccentricity
1.2
1
0.8
0.6
0.4
0.2
0
ns
ns
ns
*
*
*
si-NC
si-WNT5A
si-ZEB1-WNT5A
si-ZEB1
miR-205
miR-141
miR-200b
C
EMT phenotype score
Mesenchymal biomarkers
Epithelial biomarkers
CDH2
FN1
FOXC2
GSC
ITGB6
MMP2
MMP3
MMP9
SNAI1
SNAI2
SOX10
TWIST1
VIM
CDH1
DSP
OCLN
si-NC
si-WNT5A
si-ZEB1-WNT5A
si-ZEB1
miR-205
miR-141
miR-200b
Higher
EMT score
Mesenchyma
Epithelial
Lower
Gene expression
1.2
0.6
0.0
-0.6
-1.2

Figure 2.7. Significant changes in HEY cell morphology characteristic of MET induced by miR-200 family (miR-141/miR-200b) or miR-205 over expression are partially recapitulated by transfection with ZEB1 and/or WNT5A siRNAs. (A) Representative microscopy images after 48 h transfection with ZEB1 and/or WNT5A siRNAs or miR-141, 200b, or 205. The representative epithelial-like cells in the ZEB1 and/or WNT5A knockdown groups are circled in yellow. (B) Boxplots showing the median of cell eccentricity of ZEB1 and/or WNT5A knockdown groups is consistently lower than cell eccentricity of negative control group, but higher than the median of cell eccentricity of the miR-200 family or miR-205 over expression groups. [ns: non-statistically significant from the negative control group; asterisks: statistically significant differences from the negative control group. (*p-value < 0.05)]. (C) Heat map of gene expression (mRNA) features representing sixteen canonical EMT markers of ZEB1 and/or WNT5A knockdown groups and miR-200 family or miR-205 over expression groups. Dark blue colors represent higher expression of that gene in that sample. These features were summarized into an EMT phenotype score for each sample. Dark purple colors represent a more mesenchymal-like phenotype. Samples are ordered by high to low average EMT score.

2.4.5 Knockdown of ZEB1 and/or WNT5A induces gene expression changes in HEY cells indicative of partial MET

To determine if the apparent intermediate level of morphological changes associated with knockdown of ZEB1/WNT5A may be similarly reflected on the molecular level, we employed a previously established analytical method that assigns an EMT score based on relative gene expression levels of a 16 gene panel of canonical EMT genetic markers [67]. In order to get the expression levels of these 16 genes, we conducted microarray gene expression analyses (Affymetrix, U133 Plus 2.0 Array; Figure 2.7 C and Table A.5) as previously described [65]. Cells with higher ranked EMT scores are considered more mesenchymal-like while those with lower scores are considered more epithelial-like [67]. Consistent with the results of our morphological analyses, the ZEB1/WNT5A knockdown groups were found to display intermediate EMT scores between negative controls and the

miR-200b, miR-141, and miR-205 over-expression groups. Of the ZEB1/WNT5A knockdown groups in HEY cells, si-ZEB1 is associated with the lowest EMT score (4.19) followed by si-ZEB1-WNT5A (4.57) and si-WNT5A (4.59). Of the three miRNAs over-expressed in HEY cells, miR-200b is associated with the lowest EMT score (2.46) followed by miR-141 (3.21) and miR-205 (3.97).

2.4.6 miR-205 targets fewer EMT/MET associated genes than members of the miR-200 family suggesting an evolutionarily more recent role in the EMT/MET process

The fact that miR-205 over expression is associated with the highest EMT score of the miRNAs tested is correlated with the fact that miR-205 is predicted to target relatively fewer EMT/MET associated genes than the miR-200 family (miR-200b, miR-141) (Table A.6). Consider, for example, the representative EMT/MET pathway depicted in Figure 2.8. While miR-200b and miR-141 are predicted to directly target 30 and 28 EMT/MET pathway genes, respectively, miR-205 is predicted to target only 17 genes. Collectively, these and similar results (Table A.7) suggest that miR-205's involvement in the EMT/MET process may be evolutionarily more recent than the involvement of the miR-200 family.

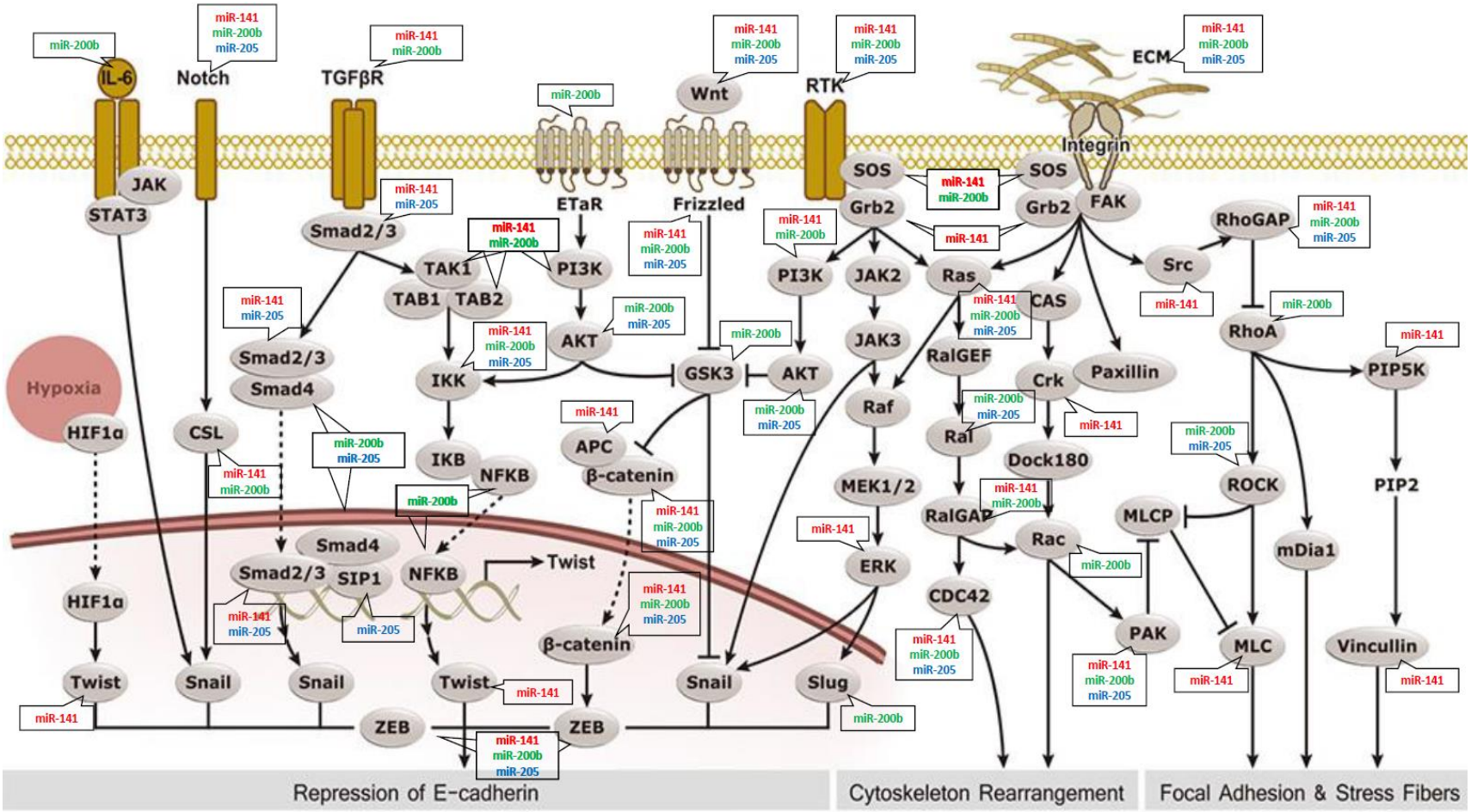

Figure 2.8. miR-200 family members (miR-141 and miR-200b) and miR-205 regulated key genes involved in EMT, invasion and metastasis pathways.

Consistent with this hypothesis, miR-200b has been shown to be involved in EMT/MET associated processes in the mouse [68, 69] while miR-205's role in mouse development is reported to be more limited in scope [70]. Moreover, while miR-200b and miR-205 are clustered together on the same chromosome in humans (human chromosome 1) placing them under similar regulatory control [71], miR-205 maps to a distinct chromosomal location (mouse chromosome 1) from miR-200b (mouse chromosome 4) in mice. Collectively, these observations suggest an evolutionarily more recent involvement of miR-205 in the EMT/MET process possibly facilitated by a chromosomal translocation event ~80 MYA (estimated time of divergence of humans and mice from a common ancestor [55].

2.5 Discussion

In principle, the induction of similar morphological changes in response to over expression of the sequentially divergent miR-200 family and miR-205 miRNAs may be explained by at least two not-mutually-exclusive hypotheses. First, if the miR-200 family and miR-205 miRNAs bind to the same mRNA (gene) target sequence(s), it could explain their coordinated regulation of the same genes. This hypothesis, however, is inconsistent with a large body of data indicating that high-sequence complementarity between miRNA seed regions and mRNA target sequence is pre-requisite to miRNA regulation [72]. Moreover, we have previously shown that even a single nucleotide substitution within the seed region of miR-200 family miRNAs is sufficient to dramatically disrupt downstream regulatory controls [9]. Thus, the high sequence divergence between miR-205 and members of the

miR-200 family of miRNAs effectively precludes the possibility that they are targeting the same mRNA binding sites.

A second, more likely scenario is that many of the genes involved in the induction of MET in HEY cells contain duplicate yet distinct target sequences for miR-200 family and miR-205 miRNAs. Indeed, it is well documented that most mRNAs (genes) contain target sequences for more than one miRNA and are thereby subject to regulatory control by multiple miRNAs [73]. Although we find that only a small percentage (<3%) of genes significantly differentially expressed in common after ectopic over expression of miR-205 or the miR-200 family of miRNAs (including genes previously implicated in EMT/MET) are predicted to be direct targets, changes in the expression of these direct targets are presumably the ultimate source of the subsequent regulatory changes, and many prior studies have confirmed the functional importance of these direct regulatory controls [45, 58]. Among genes previously implicated in the EMT process that we found to be consistently down regulated after ectopic over-expression of miR-205 or miR-200 family miRNAs in HEY cells, only *ZEB1* and *WNT5A* are predicted to be direct target genes of these miRNAs. While siRNA-mediated knock down of *ZEB1* and *WNT5A*, individually or in combination, was found to induce morphological and molecular changes characteristic of partial MET, it was not sufficient to recapitulate the changes induced by the miRNAs. This finding is consistent with an auxiliary contribution of other direct and/or indirect regulatory changes induced in common and/or individually by miR-205, miR-200b and miR-141.

The fact that miR-205 targets fewer EMT/MET associated genes than members of the miR-200 family suggests that the contribution of miR-205 to the regulation of

EMT/MET in humans is a more recent evolutionary event. We previously reported that while the seed sequence of the miR-200 family of miRNAs is highly conserved across vertebrate species, the genes targeted by these miRNAs are highly diverse [9]. This observation coupled with the finding that only a single nucleotide substitution in the target sequence (seed region) of miRNA-regulated genes can result in loss/gain of regulatory controls, led to formulation of an evolutionary model whereby individual genes may lose and/or acquire new miRNA control(s) over time through relatively minor changes in miRNA target sequence [9]. Thus, one possible explanation of the more recent contribution of miR-205 to EMT/MET trans-regulation is that it more recently acquired an expression pattern compatible with the EMT/MET process in higher vertebrates, leading to subsequent selection for the acquisition of miR-205 target sequences in EMT/MET associated genes (*e.g.*, *WNT5A*, *ZEB1*). In this regard, it is relevant to note that while miR-200b and miR-205 are clustered together on the same chromosome in humans (human chromosome 1) and display coordinated patterns of expression in apparent response to the same regulatory controls [71], in the mouse, miR-205 maps to a distinct chromosomal location (mouse chromosome 1) from miR-200b (mouse chromosome 4) placing the two miRNAs under distinct regulatory controls.

CHAPTER 3. MIRNA-MEDIATED INDUCTION OF MESENCHYMAL-TO-EPITHELIAL TRANSITION (MET) BETWEEN CANCER CELL TYPES IS SIGNIFICANTLY MODULATED BY INTER-CELLULAR MOLECULAR VARIABILITY

3.1 Abstract

Background: Ectopic overexpression of specific miRNAs has previously been reported to induce MET in a variety of cancer cells; however, the ability of individual miRNAs to induce MET when over-expressed in cancer cells is often cancer/cell-type specific.

Methods: Three sequentially divergent miRNAs previously implicated in the EMT/MET process were independently overexpressed in 3 mesenchymal-like cancer cell lines (2 ovarian/1 prostate). The molecular and phenotypic responses in each cell line were examined.

Results: The ability of these sequentially divergent miRNAs to induce MET in these cells was found to be associated with inherent differences in the starting molecular profiles of the untreated cancer cells and specifically, variability in trans-regulatory controls modulating the expression of genes targeted by the individual miRNAs.

Conclusions: While our results support the view that miRNAs have significant potential as cancer therapeutic agents, our findings further indicate that optimal treatments

will likely need to be personalized with respect to the molecular profiles of the individual cancers being treated.

3.2 Introduction

Recent years have witnessed a dramatic increase in our appreciation of the contribution of microRNAs (miRNAs) to cancer onset and progression [74]. As a consequence, there has been growing interest in the development of miRNAs not only as diagnostic biomarkers of cancer but also as a promising new class of therapeutic agents. Over the last several years, our laboratory has focused on analysis of the molecular processes underlying the ability of individual miRNAs to induce mesenchymal-to-epithelial transition (MET) particularly in ovarian cancer [64, 75-77]. Ectopic over expression of specific miRNAs down regulated during epithelial-to mesenchymal transition (EMT) have previously been reported to induce MET in a variety of cancer cells [42-44, 75], thereby reducing metastatic potential and resistance to standard-of-care chemotherapies [78, 79]. Interestingly, the ability of individual miRNAs to induce MET when over expressed in cancer cells is often cancer/cell-type specific. In an effort to better understand the molecular processes underlying this specificity, we examined the molecular and phenotypic responses of three mesenchymal-like cancer cell lines (two ovarian and one prostate) to ectopic over expression of three sequentially divergent miRNAs previously implicated in the EMT/MET process [76, 80]. The ability of these sequentially divergent miRNAs to induce MET in these cells was found to be associated with inherent differences in the starting molecular profiles of the untreated cancer cells and specifically, variability in trans-

regulatory controls modulating the expression of genes targeted by the individual miRNAs. While our results support the view that miRNAs have significant potential as cancer therapeutic agents, our findings further indicate that optimal treatments will likely need to be personalized with respect to the molecular profiles of the individual cancers being treated.

3.3 Materials and Methods

3.3.1 Cell culture and miRNA transfection

The HEY cell line was kindly provided by Gordon Mills, Department of Molecular Therapeutics, University of Texas, MD Anderson Cancer Center. SK-OV-3, and PC-3 cells were obtained from the American Type Culture Collection (ATCC, Manassas, VA). Cells were cultured in RPMI 1640 (Mediatech, Manassas, VA) supplemented with 10% FBS (Fetal Bovine Serum; Atlanta Biologicals, Lawrenceville, GA) and 1% antibiotic-antimycotic solution (Mediatech-Cellgro, Manassas, VA). For miRNA transfections, 1×10^5 cells were seeded per well in 6-well plates. Cells at exponential phase of growth were transfected with 33 nM miRNA purchased as Pre-miR miRNA Precursors (Life Technologies, Carlsbad, CA) using Lipofectamine 2000 (Life Technologies) and according to the manufacturer's instructions. Pre-miR miRNA Precursor Negative Control (Life Technologies) was used as a negative control. Cells were allowed to grow for 48 hours before RNA isolation.

3.3.2 Microarray analysis

Un-transfected cells and the transfected cells (miR-NC, miR-203a, miR-205, and miR-429) were harvested, and the RNA was extracted and subjected to microarray analysis (Affymetrix, U133 plus 2; Santa Clara, CA) as previously described [56]. Robust Microarray Averaging (RMA) was used for normalization of microarray signal and summarization using the Affymetrix Expression Console Software (Version 1.4). Statistical analysis of the expression data was carried out using the limma package executed in R [57]. Differentially expressed mRNAs were identified through adjusted p-value (FDR < 0.01) calculated using the moderated t-test.

3.3.3 miRNA target prediction

MiRNA target predictions (based on mirSVR) were downloaded from microRNA.org (August 2010 release) [59]. The mirSVR score refers to targets of microRNAs with scores obtained from the support vector regression algorithm. To reduce the occurrence of false positives, only predicted targets with a mirSVR score less than -0.1 were considered.

3.3.4 Image analysis

Morphological changes were monitored using an Olympus IX51 microscope (Olympus Optical, Melville, NY) and quantified using CellProfiler cell-imaging software (2.1.0) [62].

3.3.5 Sequence analysis of miRNA binding sites in SK-OV-3 and PC-3 cells

Full methods on whole exome sequencing (WES) sequencing and variant calling are described by Ogan et al. [81]. Briefly, 37Mb of coding region for each cell line were captured by the Agilent SureSelect All Exon v1.0 kit (Agilent, Santa Clara, CA), sequenced using the Illumina Genome Analyzer IIx instrument (Illumina, San Diego, CA), bases called via standard BWA-GATK pipeline, and followed by quality filtering as described by Ogan et al [81]. The processed exome sequencing file was downloaded from CellMiner Database (Version 2.1) [82].

Genome coordinates (hg19) of miR-203a, miR-205, and miR-429 target gene microRNA binding sequences (MBSs) were downloaded from microRNA.org [83]. To identify WES variants that were overlapping with these microRNA sites, we used customized python scripts.

3.3.6 Transcriptional repressor selection

Human transcription factor (TF)-target regulatory relationships were downloaded from the Transcriptional Regulatory Relationships Unraveled by Sentence-based Text mining (TRRUST) database [84].

3.3.7 EMT phenotype score calculation

The EMT score is generated by addition of thirteen mesenchymal-associated gene expression values and a corresponding subtraction of three epithelial-associated gene expression values to give a summary score of the EMT phenotype [67]. Cells with a high EMT score are considered more mesenchymal, whereas those with a low score more epithelial.

3.4 Results

3.4.1 The ability of miRNAs to induce morphological changes characteristic of MET is cancer cell line-dependent

Mir-429, miR-205 and miR-203a have all been previously reported to induce morphological changes characteristic of MET when ectopically over expressed in cancer cells [76, 80]. To determine the influence of individual cancer cell lines/cancer types on this process, we ectopically over expressed each of these miRNAs in two individually derived ovarian cancer (OC) cell lines (HEY [85], SK-OV-3 [86]) and one prostate cancer (PC-3) [87] cell line. All of these cell lines display a starting elongated mesenchymal-like morphology but respond differently within 48 h of ectopic over expression of each of the three miRNAs relative to a synthetic negative control miRNA. We quantified morphological differences existing between the three cell types before and after ectopic over expression of the three miRNAs using CellProfiler cell-imaging software (2.1.0) [88]. The results (Figure 3.1) indicate that un-transfected HEY cells display the most elongated, mesenchymal-like morphology followed by PC-3 cells and SK-OV-3 cells, which displayed a relatively more rounded, epithelial-like morphology.

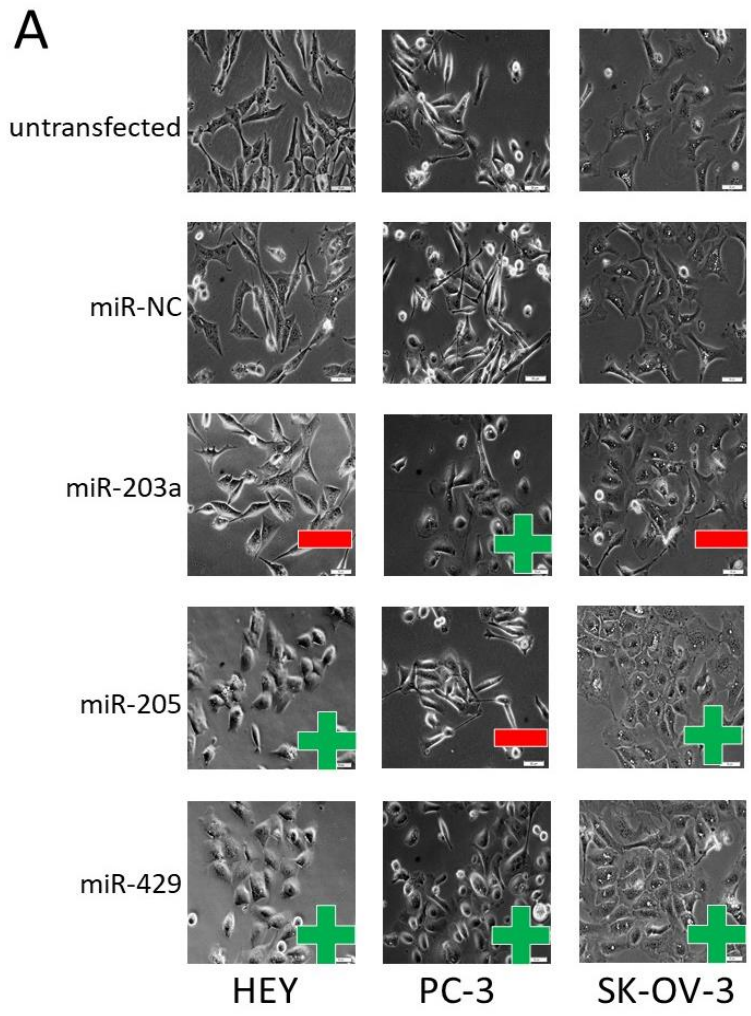
A
untransfected
miR-NC
miR-203a
miR-205
miR-429
HEY
PC-3
SK-OV-3

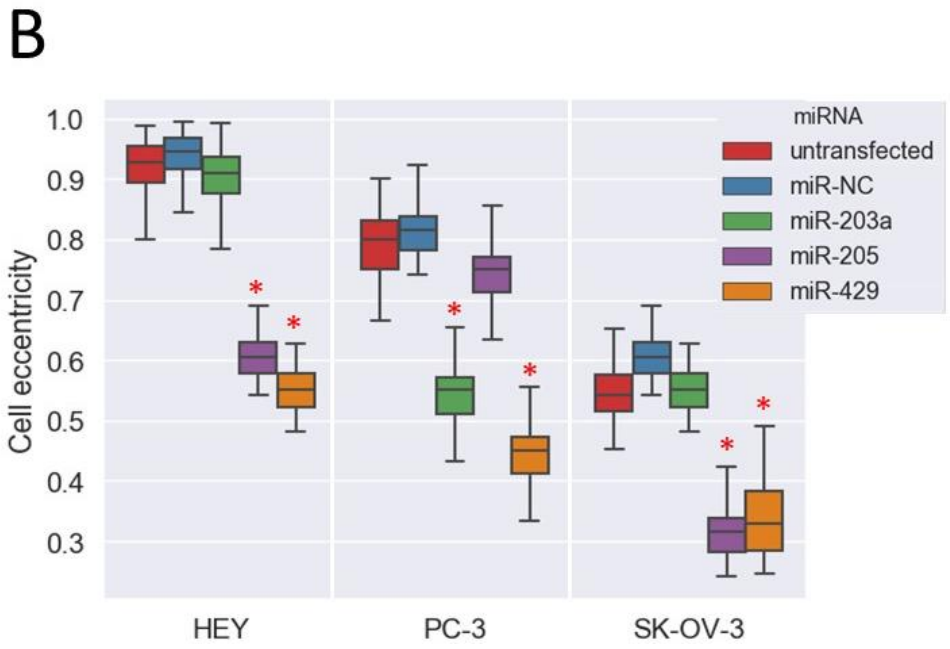
B
Cell eccentricity
1.0
0.9
0.8
0.7
0.6
0.5
0.4
0.3
miRNA
untransfected
miR-NC
miR-203a
miR-205
miR-429
HEY
PC-3
SK-OV-3

Figure 3.1. Comparison of morphological changes induced by over expression of the same suite of miRNAs (miR-203a, miR-205, and miR-429) in mesenchymal-like cells (HEY, SK-OV-3, and PC-3 cells). (A) Representative microscopic images (20X) of untransfected and transfected cells (48 h post-transfection with miRNAs; scale bars, 50 µm; "+" = MET; "-" = no MET). (B) The accumulation of a more rounded epithelial-like cells occurred in miR-429/205 transfected ovarian cancer cells (HEY and SK-OV-3 cells) and miR-429/203a transfected prostate cancer cells (PC-3 cells) 48 h post-transfection (cell eccentricity: a score of 0 = circular shape, a score of 1 = linear shape). Significance of differences is evaluated using Student's t-test. (compared to miR-NC, p-value < 0.05).

Over expression of miR-205 induced a significant morphological change to a more rounded/cuboidal phenotype consistent with MET in the two OC cell lines (HEY and SK-OV-3) but not in the prostate cancer cell line (PC-3) relative to negative controls. In contrast, miR-203a induces morphological changes characteristic of MET in PC-3 cells but not in the HEY and SK-OV-3 cells, while miR-429 induces morphological changes characteristic of MET in all three of the cell lines.

3.4.2 Ectopic over expression of miR-203a, miR-205 and miR-429 induced both direct and indirect changes in gene expression in HEY, SK-OV-3 and PC-3 cells

To explore the molecular level changes induced by ectopic over expression of each of the three miRNAs in the three cell lines, we extracted RNA from each of the cell lines 48 h after over expression of each of the three miRNAs and corresponding negative controls. RNA samples were collected from each of the three cell lines with three replicates of five treatments (miR-203a, miR-205, miR-429, miR-NC, un-transfected) for a total of 45 samples (3 cell lines X 5 treatments X 3 replicates). Initial quality control, summarization

and normalization of the 45 CEL files using RMA (Robust Multiarray Average) was performed using the Affymetrix Expression Console as previously described [64]. The result was expression data for 23,031 annotated genes (Table B.1).

Ectopic over expression of the three miRNAs resulted in significant changes in gene expression in each of the cell lines (Figure 3.2A). Consistent with previous studies [77], we found that on average 21.3% of genes differentially expressed in response to miRNA over expression are predicted to be direct targets of the respective miRNAs (HEY: miR-203a, 491/1764 = 27.8%, miR-205,1443/11,123 = 13.0%, miR-429, 1956/9395 = 20.8%; SK-OV-3: miR-203a, 381/882 = 43.2%, miR-205, 875/6500 = 13.5%, miR-429, 1385/6925 = 20.0%; PC-3: miR-203a, 1846/8320 = 22.2%, miR-205, 1184/9779 = 12.1%, miR-429, 948/4928 = 19.2%; Figure 3.2B). The observed changes in gene expression are also consistent with prior evidence that the majority of changes induced by ectopic over expression of miRNAs are indirect, albeit initiated by changes in directly targeted genes [89].

While a notable fraction of the changes in gene expression were induced in common in the three cell lines, the majority of differentially expressed genes were unique to each miRNA-cell type combination (Figure 3.2). This was most pronounced for miR-203a in PC-3 cells where 84.1% of differentially expressed genes did not overlap with those induced in HEY or SK-OV-3 cells. Interestingly, PC-3 was the only one of the three cell lines displaying MET in response to miR-203a over expression suggesting that at least some of the non-overlapping genes may be critical to miR-203a induced MET in this cell line.

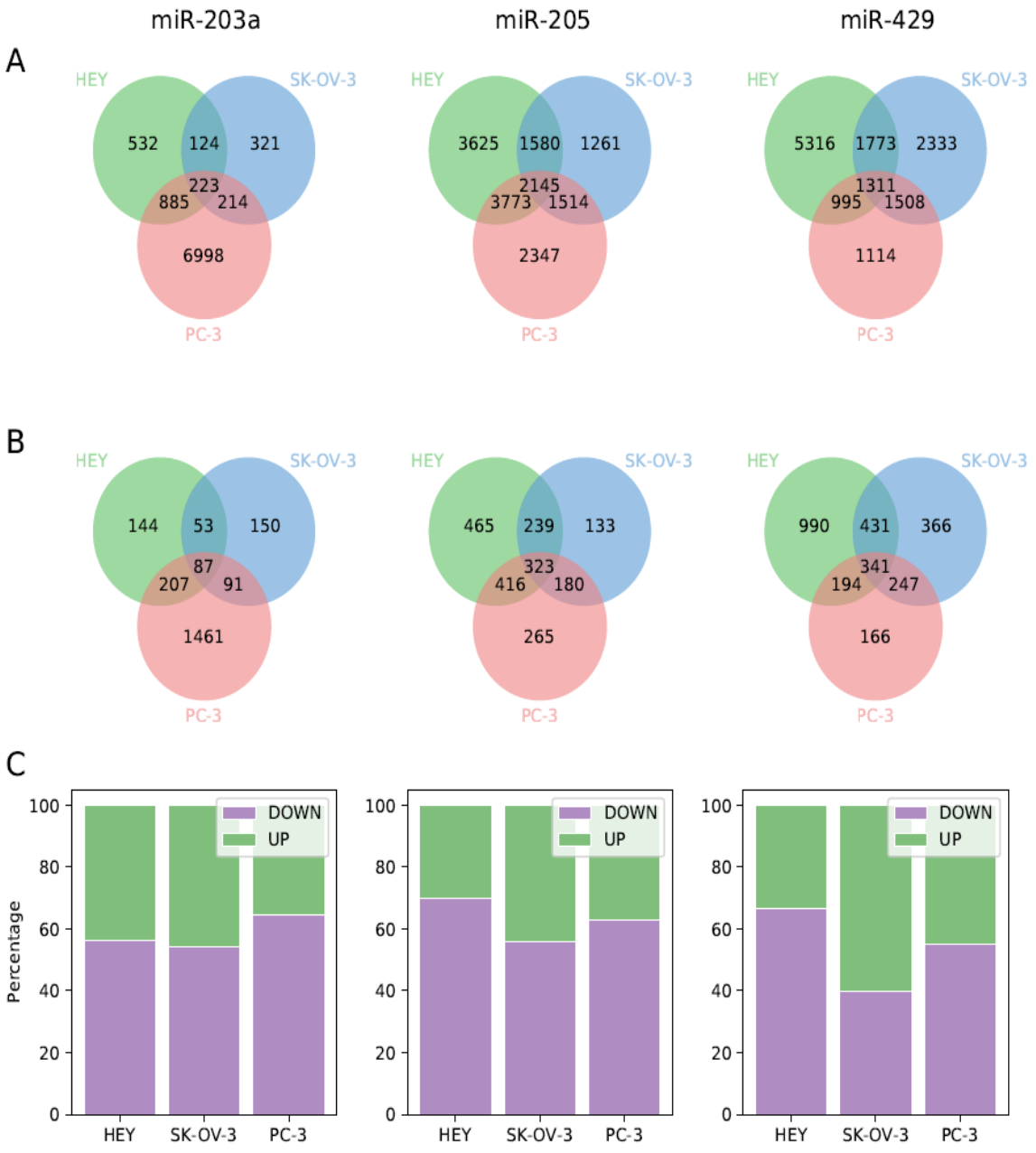

Figure 3.2. Analysis of differentially expressed genes after transfection of the same suite of miRNAs (miR-203a, miR-205, and miR-429). (A) Venn diagram showing the intersection of all differentially expressed genes after over expression of miR-203a, miR-205, and miR-429 individually in HEY, SK-OV-3, and PC-3 cells. (B) Venn diagram showing the intersection of differentially expressed direct target genes after individual over expression of miR-203a, miR-205, and miR-429 in HEY, SK-OV-3, and PC-3 cells. (C) Histogram showing the percentage of the up-regulated and down-

regulated direct target genes in differentially expressed genes after individual over expression of miR-203a, miR-205, and miR-429 in HEY, SK-OV-3, and PC-3 cells. Significantly differentially expressed genes between treatments were selected at an adjusted (Benjamini-Hochberg) limma p-value of 0.01.

3.4.3 The unexpected response of some miRNA targeted genes may be at least partially explained by transcriptional override

With the notable exception of miR-429 in SK-OV-3 cells, the majority of the miRNA directly targeted genes displaying significant changes in expression were down regulated consistent with RISC (RNA-induced silencing complex)-mediated regulation of targeted genes by miRNAs [90] (Figure 3.2C). No change or up regulation of target genes after over expression of miRNAs has been observed previously [91, 92] and may, at least in part, be explained by the transcriptional override model (TOM) [93].

TOM postulates that the expected down regulation of target genes induced by elevated levels of regulating miRNAs may be masked or "overridden" by increases in transcriptional initiation mediated by the down regulation of repressor genes that are themselves targets of the same regulating miRNAs. Depending upon the strength of the transcriptional override (*i.e.*, the relative strengths of miRNA and repressor gene mediated de-repression), TOM predicts that increases in miRNA levels may display no effect or be positively correlated with changes in levels of their targeted mRNAs.

To determine if TOM may at least partially explain the differential responses of our cell lines to over expression of the same miRNAs, we downloaded from the TRRUST (Transcriptional Regulatory Relationships Unraveled by Sentence-based Text mining)

database [84], a list of transcription factors (TFs) thus far identified as repressors of those genes we observed to display no change or to be up regulated after ectopic over expression of the three miRNAs. From among these TFs, we further selected those repressor genes predicted to be targets of the same three over expressed miRNAs and that responded by displaying a significant down regulation in expression (see "Repressor Expression" in Table B.2-4). Combining this dataset with predicted gene targets [83] (of the same miRNAs) that displayed no change or were up regulated after miRNA ectopic over expression, allowed us to identify genes displaying responses consistent with TOM (Table 3.1, Table B.2-4).

Table 3.1. miRNA-mediated de-repression of repressor genes overrides the expected down-regulatory effects of miRNAs on their target gene expression.

	miR-203a		**miR-205**		**miR-429**	
	Repressor (D)	**Target (NC, U)**	**Repressor (D)**	**Target (NC, U)**	**Repressor (D)**	**Target (NC, U)**
HEY	8	21	12	11	19	26
SK-OV-3	19	36	6	9	13	21
PC-3	19	33	12	13	13	23

*: D, U, NC: significantly up-regulated, significantly down-regulated, non-significantly changed after overexpression of corresponding miRNA.

In total, 105 target genes were found to display up regulation or no change in expression in response to miRNA over expression consistent with TOM (Table B.2-4). For illustrative purposes, Figure 3.3 displays those targeted genes displaying up regulation in expression in response to over expression of their regulating miRNA consistent with TOM. For example, *CDH1* (cadherin 1), a gene recognized as playing a central role in EMT/MET [94], is a direct target of miR-205 and yet was observed to be significantly up regulated

after ectopic over expression of miR-205. Interestingly, the repressor protein ZEB1, known to play a central role in EMT/MET [95], is also a direct target of miR-205 and a known regulator of CDH1 [96]. Thus, consistent with TOM, miR-205 down regulation of ZEB1 may be overriding the regulatory effect of miR-205 on CDH1 expression.

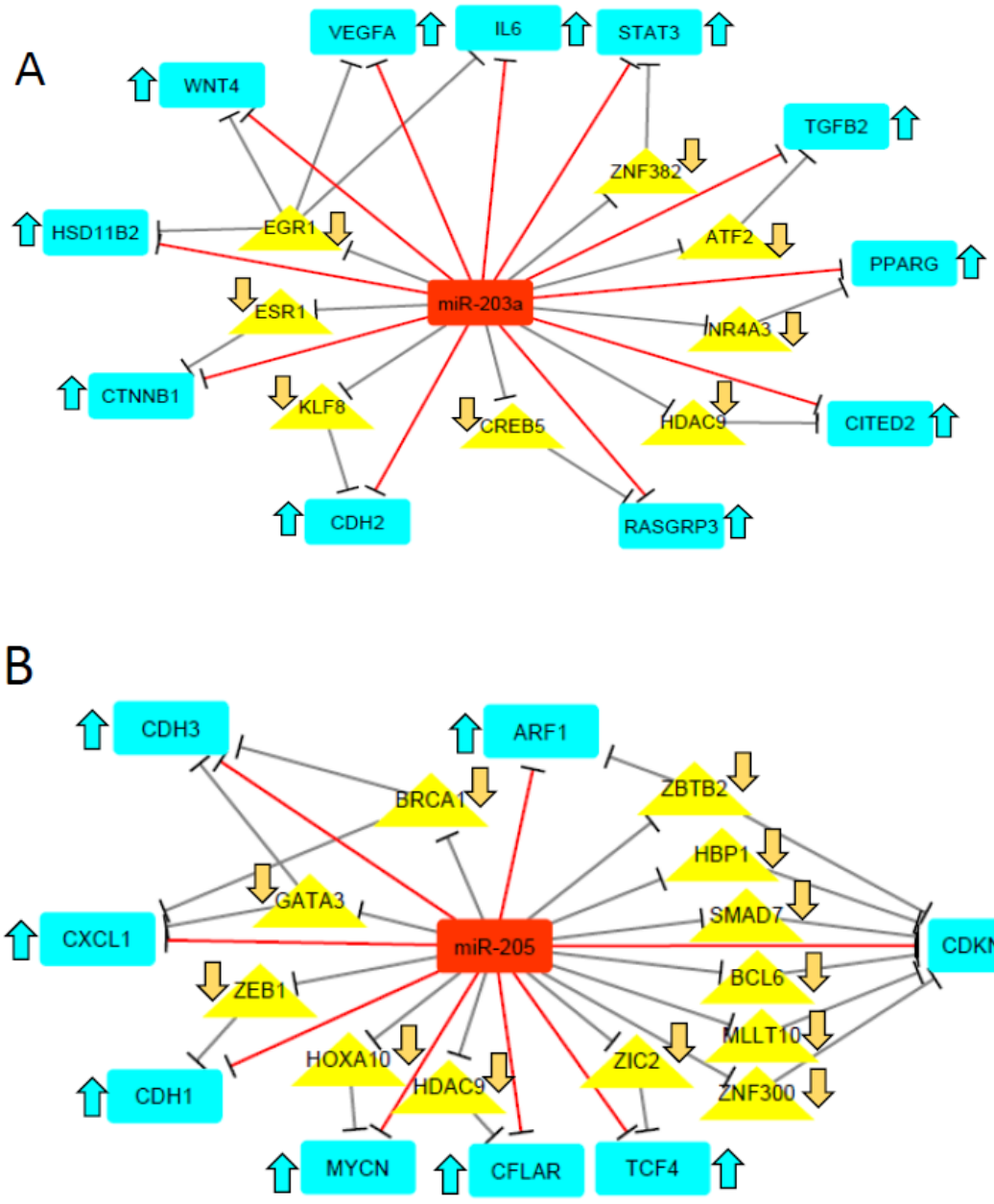

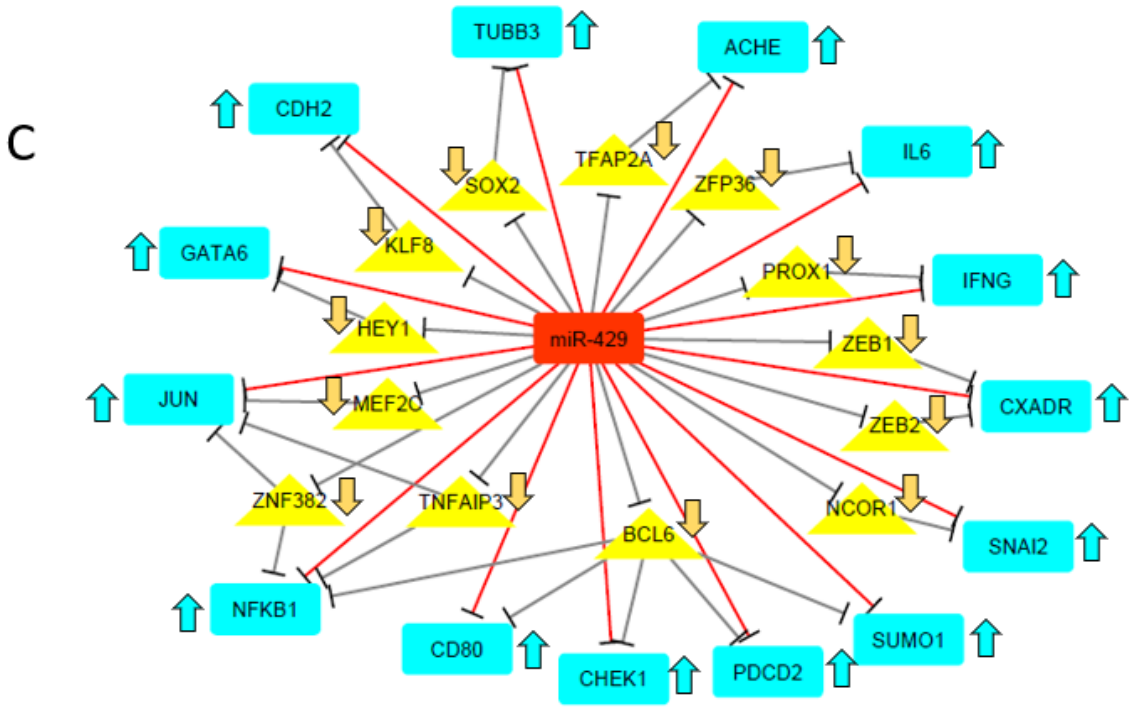

Figure 3.3. miRNA-mediated de-repression of repressor genes (yellow triangles) may override the expected down-regulatory effects of miRNAs (red squares) on their target gene (blue squares) expression. (A) miRNA-203a, (B) miR-205, (C) miR-429 mediated de-repression. (A) miRNA-203a, (B) miR-205, (C) miR-429 mediated de-repression of down-regulated repressor genes overrides the expected down-regulatory effects of miRNA, resulting in up regulation in miRNA target gene expression. The overridden down-regulatory effects of miRNAs on their target genes have been marked in red. (Direction of observed changes in gene expression in response to miRNA over expression indicated by arrows)

3.4.4 Expression of genes previously associated with EMT/MET are significantly changed in response to overexpression of miR-203a, miR-205 and miR-429 in a cell-line specific manner

We next focused on 84 genes previously identified as being directly or indirectly associated with the EMT/MET process in one or more cellular contexts (Table B.5) [97-100]. Ectopic

over expression of each of the three miRNAs induced variable patterns of change in the expression of these EMT/MET associated genes across the three cell lines (Figure 3.4A).

In contrast to what was found for all differentially expressed as well as direct target genes (Figure 3.2), the majority of differentially expressed EMT/MET-associated genes were expressed in common in each miRNA-cell type combination (Figure 3.4). This change in expression pattern may be a reflection of selective enrichment in the targeting of EMT/MET genes by all of the miRNAs.

The notable exception is for genes induced by miR-203a over expression in PC-3 where 50% of the changes in gene expression were unique to PC-3 cells. Again, it is interesting to note that PC-3 cells were the only one of the three cell lines displaying MET in response to miR-203a over expression. The observed changes in gene expression in EMT/MET-associated genes that were cell line/miRNA-specific in this and the other cell lines underscores the importance of genetic background on the response of cells to miRNA regulation.

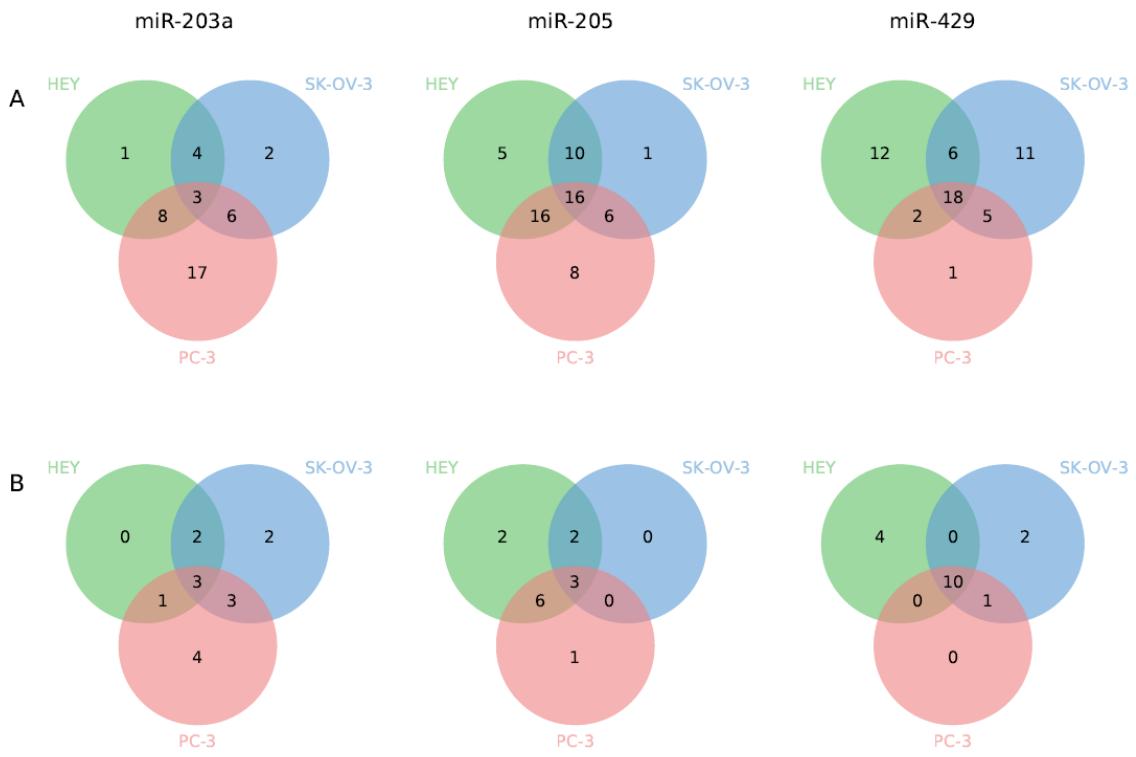

Figure 3.4. Analysis of differentially expressed EMT/MET genes after transfection of the same suite of miRNAs (miR-203a, miR-205, and miR-429). (A) Venn diagram showing the intersection of differentially expressed EMT/MET-associated genes after over expression of miR-203a, miR-205, and miR-429 individually in HEY, SK-OV-3, and PC-3 cells. (B) Venn diagram showing the intersection of differentially expressed directly targeted EMT/MET-associated genes after over expression of miR-203a, miR-205, and miR-429 individually in HEY, SK-OV-3, and PC-3 cells. Significantly differentially expressed EMT/MET-associated genes between treatments were selected at an adjusted (Benjamini-Hochberg) limma p-value of 0.01.

3.4.5 The relative level of changes in cellular morphology induced by miRNA overexpression is correlated with changes in levels of expression of molecular biomarkers of EMT/MET

To determine if differences in the level of morphological change induced by miRNA over expression in the three cell lines (Figure 3.1) is similarly reflected on the molecular level,

we employed a previously established analytical method that assigns EMT scores based on the relative gene expression levels of a panel of 16 canonical EMT genetic markers [67]. Cells with higher EMT scores are considered more mesenchymal-like while those with lower scores are considered more epithelial-like. Consistent with the results of our morphological analyses (Figure 3.1), HEY cells displayed the highest (most mesenchymal-like) EMT score followed by PC-3 and SK-OV-3 cells, which displayed the lowest EMT score (most epithelial-like) (Figure 3.5).

A

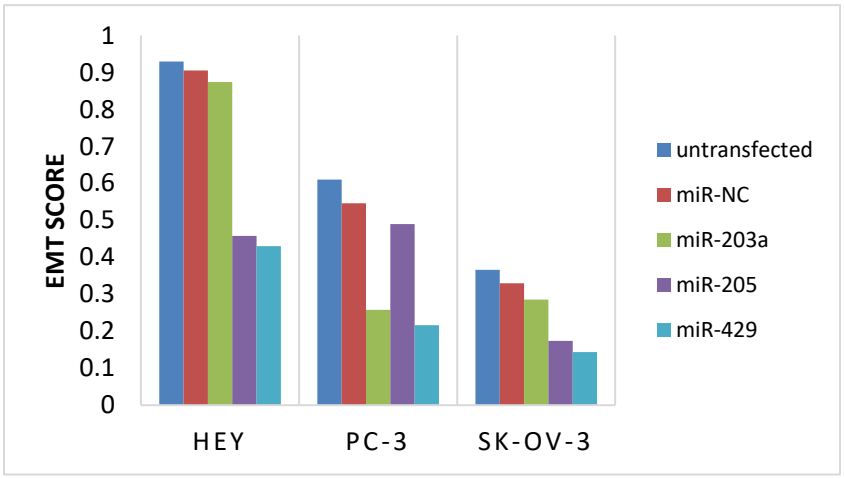

B

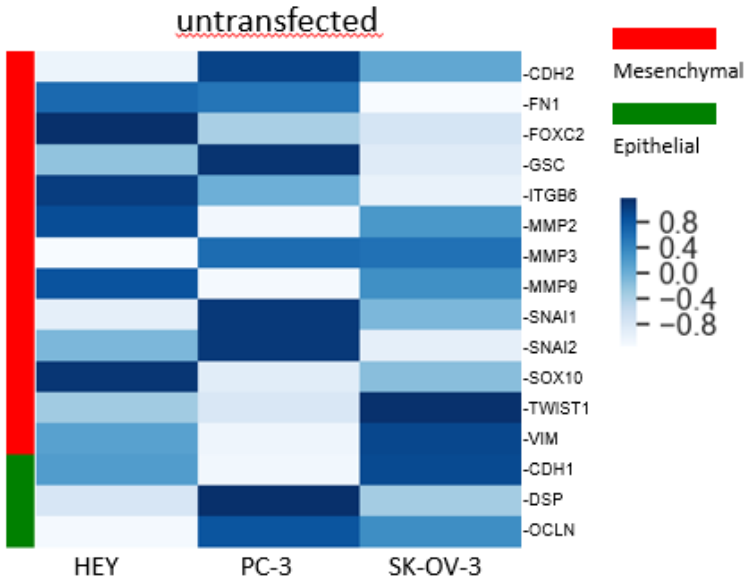

C

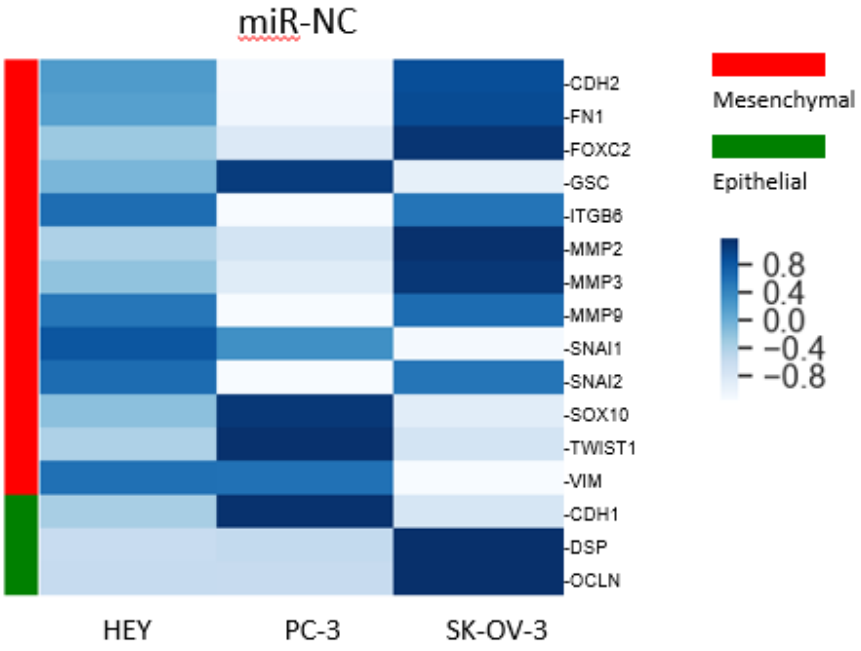
miR-NC
CDH2
FN1
FOXC2
GSC
ITGB6
MMP2
MMP3
MMP9
SNAI1
SNAI2
SOX10
TWIST1
VIM
CDH1
DSP
OCLN
HEY
PC-3
SK-OV-3
Mesenchymal
Epithelial
0.8
0.4
0.0
−0.4
−0.8

D

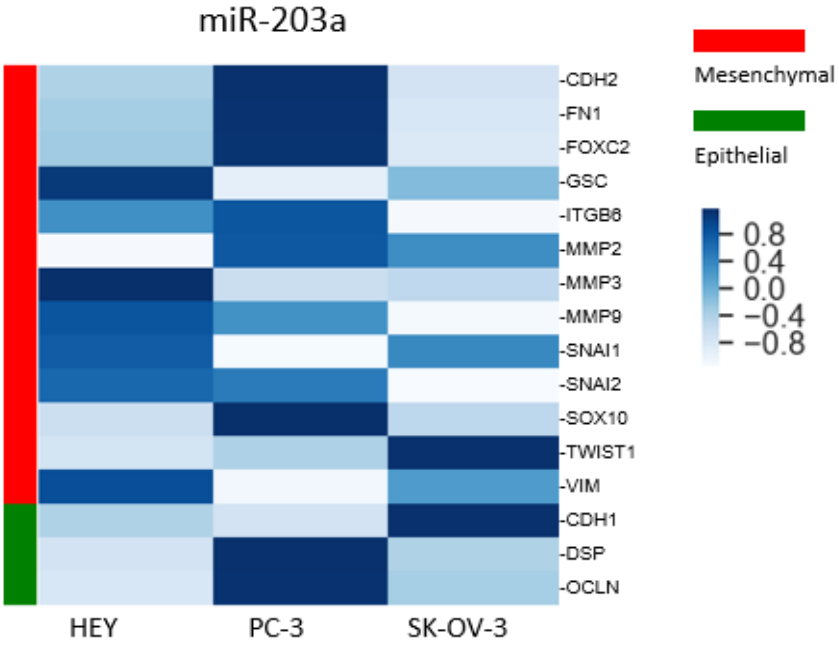
miR-203a
CDH2
FN1
FOXC2
GSC
ITGB6
MMP2
MMP3
MMP9
SNAI1
SNAI2
SOX10
TWIST1
VIM
CDH1
DSP
OCLN
HEY
PC-3
SK-OV-3
Mesenchymal
Epithelial
0.8
0.4
0.0
−0.4
−0.8

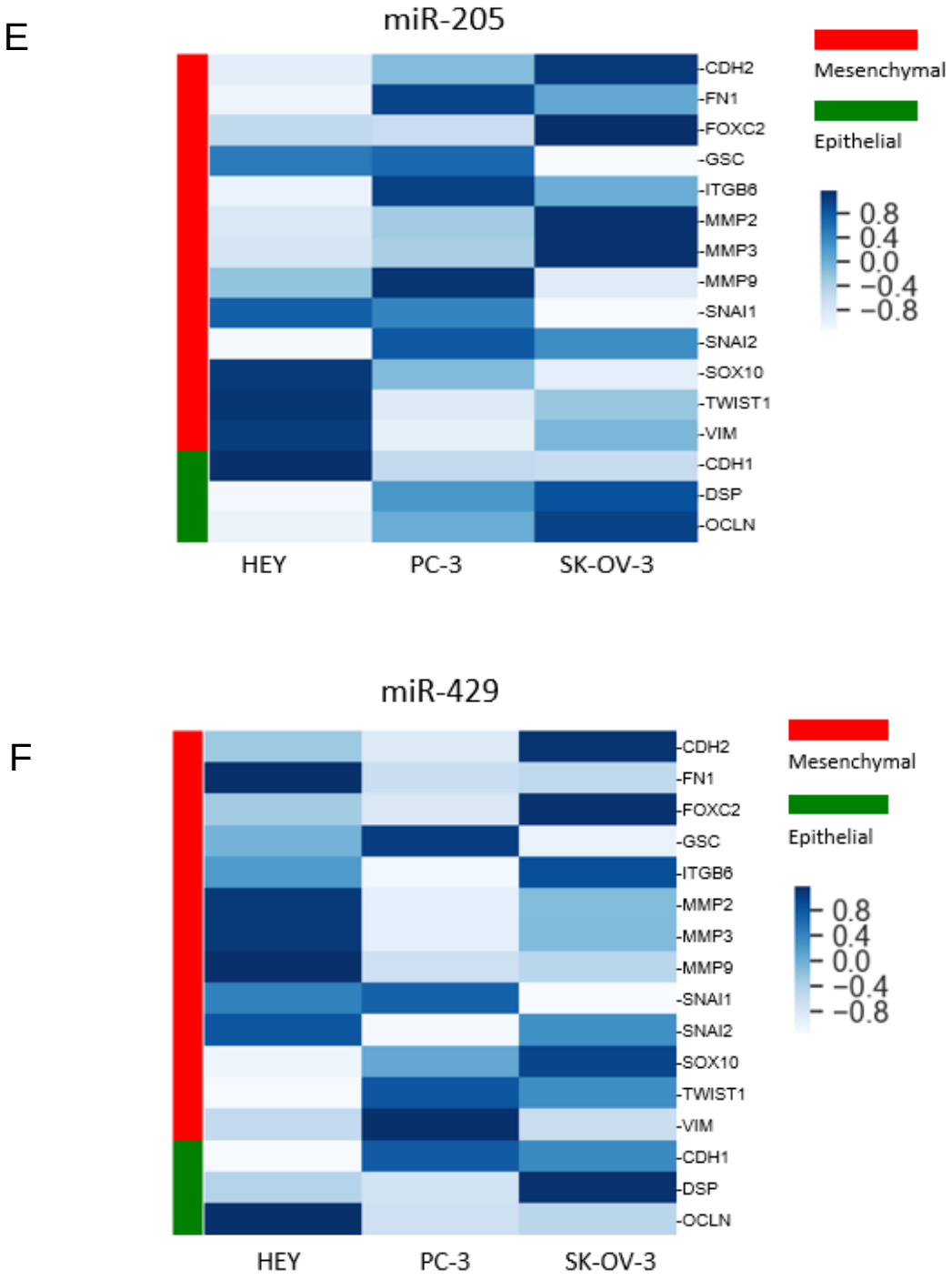

Figure 3.5. Comparison of EMT score changes after transfection of the same suite of miRNAs (miR-203a, miR-205, and miR-429) in HEY, SK-OV-3, and PC-3 cells. (A) Histogram showing EMT scores in untransfected and transfected (miR-NC, miR-203a, miR-205, and miR-429) HEY, PC-3, and SK-OV-3 cells. (B-F) Heatmap of gene expression features representing canonical EMT markers in untransfected (B), miR-

NC transfected (C), miR-203a transfected (D), miR-205 transfected (E), and miR-429 transfected (F) HEY, PC-3, and SK-OV-3 cells.

We next computed changes in EMT scores for each of these three cell lines after ectopic over expression of the three miRNAs relative to negative controls. The results (Figure 3.5) demonstrate that miRNA-induced changes in morphology (Figure 3.1) correlate well with changes in EMT scores. Over expression of miR-203a induced a reduction in EMT score in PC-3 cells but no change in HEY or SK-OV-3 cells. In contrast, over expression of miR-205 induced a reduction in EMT scores in HEY and SK-OV-3 cells, but no change in PC-3 cells. Over expression of miR-429 induced a major change in EMT scores in all three of the cell lines tested.

Interestingly, there were significant differences among the cell lines in the morphological (Figure 3.1) and EMT score end points acquired in response to over expression of the miRNAs. For example, the end points in morphology and EMT score levels acquired in response to over expression of miR-205 or miR-429 in HEY cells are greater than in SK-OV-3 cells. Indeed, the end point responses for Hey cells are approximately equal to the starting point (negative control) of the SK-OV-3 cells. Likewise, the morphological and EMT score levels acquired in response to over expression of miR-203a in PC-3 cells are approximately equivalent to the starting (negative control) levels of SK-OV-3 cells. These results indicate that differences in the genetic background between each of the three cell lines not only play a significant role in determining the cellular response to over expression of each of the individual miRNAs but in the magnitude of the induced response as well.

3.4.6 Changes in the miRNA-induced expression patterns of EMT/MET-associated genes correlate with induced changes in morphology and EMT scores

Of the 84 genes previously implicated in the EMT/MET process, some have been previously identified as being typically up regulated during EMT (*i.e.* down regulated during MET) and others typically down regulated during EMT (*i.e.* up regulated during MET) (Table B.5) [97-100]. In an effort to identify those EMT/MET-associated genes that may be contributing to the differential response of the cell-lines to miRNA over expression, we sought to identify genes targeted by the over-expressed miRNAs that display changes in levels of expression consistent with the miRNA-induced changes in morphology and correlated EMT scores (Table B.6-8). For example, repressor gene *ZEB1* previously has been shown to be expressed at relatively lower levels in epithelial-like cells and relatively higher levels in mesenchymal-like cells [75, 101]. Since ZEB1 is a direct target of miR-429, the expression of ZEB1 is expected to be down regulated in each of the three mesenchymal-like cell lines displaying morphological changes characteristic of MET. Consistent with this prediction, ZEB1, as well as its paralog ZEB2, and three other direct targets of miR-429 (FN1, MSN, ITGAV) previously associated with high expression in mesenchymal-like cells were significantly down regulated in all three cell lines in response to miR-429 over expression (Table B.8). In addition, four other EMT/MET genes previously associated with high expression in mesenchymal-like cells, but not direct targets of miR-429, were also significantly down regulated, again underscoring the apparent importance of indirect miRNA-induced regulatory changes in EMT/MET.

In contrast to miR-429, over expression of miR-205 was observed to induce MET in HEY and SK-OV-3 cells but not in PC-3 cells. Consistent with the miR-205-induced changes in morphology/EMT scores, EMT/MET genes previously associated with high expression in mesenchymal-like cells were significantly down regulated in HEY and SK-OV-3 cells, but displayed either no significant change in expression (*ZEB 2*, *PTP4A1*) or were significantly up regulated (*TCF4*, *GNG11*) in PC-3 cells (Table B.7).

Over expression of miR-203a induced changes in morphology and in EMT scores in PC-3 cells but not in HEY or SK-OV-3 cells. Consistent with these observations, nineteen EMT/MET genes displayed correlated changes in expression characteristic of MET in PC-3 cells but no correlated change in expression in HEY or SK-OV-3 cells (Table B.6).

Of the 27 EMT/MET genes displaying changes in patterns of expression correlated with the miRNA-induced changes in morphology/EMT scores, only five (*ZEB1*, *ZEB2*, *GNG11*, *TCF4*, *KRT19*) were responsive to more than one of the over expressed miRNAs. This observation coupled with the fact that the majority of the 84 EMT/MET genes did not display significant changes in expression correlated with the miRNA-induced changes in morphological/EMT scores, is consistent with prior evidence that molecular changes underlying EMT/MET can vary significantly between individuals and cell types [102].

3.4.7 Variability in the response of HEY, SK-OV-3 and PC-3 cells to miRNA over expression likely involves differences in cell-specific trans-regulatory controls

A major factor in the regulation of genes by miRNAs is the degree of complementarity between the miRNA sequence (especially the 7-8 nucleotide "seed region") and one or more "target sequences" typically located within the 3' untranslated region (UTR) of regulated genes. For example, we have previously shown that even a single nucleotide change within the seed region of the miR-200 family of miRNAs is sufficient to significantly disrupt regulatory control of target genes expression [9]. Thus, one possible explanation of the differential regulatory response of genes to over expression of the same miRNA in different cells types is sequence variation between cells in the miRNA target sequences of regulated genes. To explore the possibility that such sequence variation may be contributing to the differential response of target genes to miRNA over expression in SK-OV-3 and PC-3 cells, we downloaded processed whole exome sequencing files of NCI-60 cell lines from CellMiner database [103] (Note that HEY cells are not one of the NCI-60 cell lines and thus sequence data are unavailable).

Sequence comparison of the 3’ untranslated regions (UTRs) of target genes differentially responding to over expression of the same miRNA in PC-3 and SK-OV-3 cells (from genes listed in Table B.6-8) failed to uncover any sequence variation between the cell lines in miRNA target regions (Table B.9). Thus, in so far as sequence variation within the 3’ UTRs between SK-OV-3 and PC-3 cells is representative, it appears that variation in the miRNA target sequences of regulated genes is unlikely to be a primary cause of the differential regulatory response of genes to over expression of the same miRNA in different cell lines.

An alternative explanation of the differential response of target genes to over expression of the same miRNAs in different cells is cell-specific variation in trans-regulatory controls capable of directly or indirectly modulating the action of miRNAs. For example, ectopic over expression of miR-203a results in down regulation of its target gene *SNAIL2* in HEY and SK-OV-3 cells but not in PC-3 cells (Table B.10). Two known repressors of SNAIL2 (CREB1 and SUZ12) are down regulated in PC-3 cells but not in HEY and SK-OV-3 cells possibly negating/overriding the down-regulatory effect of miR-203a over expression on SNAIL2 in PC-3 cells. Other scenarios are possible and will become better defined as our understanding of the complexities of variation in gene-gene regulatory interactions between cells becomes better understood.

3.5 Discussion

MiRNAs are widely recognized as a major component of post-transcriptional regulatory control in eukaryotes [104]. Modulations in the expression of miRNAs have been associated with a variety of diseases [105] including cancer where they are being developed as biomarkers of early disease onset [106] , as well as, a potential new class of therapeutic agents [107]. The observation that there can be considerable variation in the functional consequence of ectopic over expression of the same miRNAs in different cell lines emphasizes the importance of host cell-miRNA interactions, as well as, the importance of understanding of the molecular basis of this phenomenon as a pre-requisite to clinical application.

In an effort to better understand and characterize the molecular basis of host cell-miRNA interactions, we systematically studied the morphological and molecular consequences of ectopic over expression of three sequentially divergent miRNAs previously implicated in the EMT/MET process in three distinct mesenchymal-like cancer cell lines. Two of these cell lines were derived from ovarian cancers (HEY and SK-OV-3) and the other was derived from a prostate cancer (PC-3). Whole transcriptome microarray profiling established that an average of 6624 genes were significantly differentially expressed in each of the cell lines in response to ectopic over expression of each of the three miRNAs. Consistent with earlier results, only a minority of these differentially expressed genes was found to be direct targets of the miRNAs. This finding demonstrates that changes in miRNA expression levels trigger a cascade of cellular responses extending well beyond those induced in directly targeted genes. Indeed, on average 21.3% of the significantly differentiated genes are predicted to be directly targeted by one or other of the three miRNAs.

Consistent with earlier studies demonstrating that the transition from an epithelial to mesenchymal cell type (EMT) is a graded, step-wise process [102], we found significant differences between the three cells lines in morphological and molecular indices of cell type. Although all three cell lines have previously been described as mesenchymal-like, HEY cells were found to display the most elongated morphology and pronounced mesenchymal molecular index. PC-3 cells were found to be intermediate both morphologically and on the molecular level, while SK-OV-3 cells displayed the most epithelial-like morphologies and molecular profiles.

Ectopic over expression of the three miRNAs in each of the cell lines resulted in remarkedly different results. Over expression of miR-429 induced significant morphological and molecular changes characteristic of MET in all three cell lines. In contrast, over expression of miR-205 resulted in significant changes in these parameters in HEY and SK-OV-3 cells but not in PC-3 cells, while over expression of miR-203a resulted in morphological and molecular changes characteristic of MET only in PC-3 cells. These results suggest that differential responses to future miRNA-based therapies should be anticipated not only between different types of cancer but perhaps in different patients with the same cancer as well.

In an effort to explore the possible molecular basis of the varied responses of different cells to the same miRNA treatment, we focused on a set of genes previously identified as being directly or indirectly involved in EMT/MET in one or another cellular context. As was the case for all differentially expressed genes, only a minority of the EMT/MET genes was predicted to be direct targets of the miRNAs, again underscoring the importance of indirect changes induced in response to modulations in miRNA expression. In contrast to what was found for all differentially expressed direct and indirectly targeted genes, the majority of differentially expressed EMT/MET-associated genes were expressed in common in each miRNA-cell type combination. This is likely a reflection of selective enrichment in the targeting of EMT/MET genes by these MET-inducing miRNAs.

To identify EMT/MET genes that may be directly contributing to the differential response of the cell-lines to miRNA over expression, we identified 27 genes directly

targeted by the over expressed miRNAs that displayed changes in levels of expression consistent with the miRNA-induced changes in morphology and correlated EMT scores. Only five of these 27 genes were similarly responsive to the over expression of each of the three miRNAs consistent with earlier evidence that the drivers of EMT/MET can vary significantly between cells. Also consistent with this view is the fact that the majority of the 84 EMT/MET genes did not display changes in expression correlated with the miRNA-induced changes in morphological/EMT scores in any of the three cell lines examined. Based on comparative sequence analysis of the target sequences of miRNA regulated genes in SK-OV-3 and PC-3 cells, we conclude that the molecular basis of the variable response of different cell lines to miRNA over expression is likely not primarily attributable to variation in *cis*-regulatory sequences in the UTR of targeted genes but rather to cell-specific variation in genes that can modulate the action of miRNAs.

Collectively our results indicate that miRNA-mediated regulation of EMT/MET, like other pathways implicated in cancer onset and progression [108], is a highly integrated process that can be significantly modulated by the molecular background of different cells. The overall clinical implication of our study is that the future utility of any given miRNA in cancer diagnostics and therapeutics is likely to be cancer-type and possibly individual patient dependent, reinforcing the importance of a personalized approach to cancer medicine [109-111].

CHAPTER 4. EVIDENCE FOR THE IMPORTANCE OF POST-TRANSCRIPTIONAL REGULATORY CHANGES IN OVARIAN CANCER PROGRESSION AND THE CONTRIBUTION OF MIRNAS

4.1 Abstract

Objective: To explore the relationship between RNA and protein expression in the context of ovarian cancer metastasis by systematically comparing of the expression of 4436 genes on the RNA and protein levels between primary and metastatic samples collected from the same ovarian cancer patient.

Methods: Cancer cells were isolated from bulk primary and metastatic (omentum) tissues by laser capture microdissection. mRNA expression was measured by microarray and protein expression a highly sensitive mass spectrophotometric method.

Results: The overall correlation between changes in levels of mRNA and their encoding proteins is low (r=0.38). The majority of changes in levels of expression are on the protein level with no corresponding change on the mRNA. Computational and experimental evidence demonstrates that a significant fraction of the discordant changes in levels of RNA and protein between primary and metastatic cancer samples is mediated by microRNAs. The majority (>60%) of changes in RNA and protein levels between the primary and metastatic samples of the same ovarian cancer patient are not correlated underscoring the limitations of functional pathway predictions based on RNA profiling alone. Indirect and direct evidence indicates that much of the observed discordance may be attributed to changes in miRNA expression.

Conclusions: Our findings are consistent with growing evidence of the importance of post-transcriptional/translational changes in the onset and progression of ovarian and other cancers and the significance of miRNAs in regulating the process.

4.2 Introduction

The last several decades have witnessed historic breakthroughs in the development of new high-throughput technologies to detect molecular changes associated with cancer onset and progression. The detection of these molecular changes, combined with appropriate computational methods, has proven extremely useful in the establishment of highly accurate diagnostic markers of the disease [74, 75]. The functional significance of the detected changes has proven more difficult to interpret because of our limited understanding of the underlying causal mechanisms involved [76]. A case in point is the relationship between changes in levels of RNA transcripts and corresponding changes (or lack thereof) in levels of their encoded proteins [77]. For example, high-throughput technologies have identified significant changes in patterns of mRNA expression between cancer patient primary and metastatic samples but the functional significance of these changes often rests upon the assumption that observed changes in levels of mRNA accurately reflect changes in levels of their encoded proteins [78, 79]. The validity of this assumption is far from confirmed and is, in fact, questionable in light of increasing evidence of the importance of post-transcriptional mechanisms in both the onset and progression of many cancers [80, 81].

We report here the results of a systematic comparison of the expression of 4436 genes on the RNA and protein levels between tumor samples collected from the ovary (OV) and omentum (OM) of same ovarian cancer (OC) patient. Consistent with other recent studies [82-84], our results indicate that the overall correlation between differences in levels of mRNA and their encoding proteins is low (r=0.38). We find that the majority of the differences in levels of expression are on the protein level with no corresponding change on the mRNA level implying the importance of post-transcriptional regulatory mechanisms. The results of gene ontology (GO) analyses further support this conclusion. Finally, we present evidence that a significant fraction of the discordant differences in levels of RNA and protein between the OV and OM cancer samples is mediated by microRNAs.

4.3 Materials and Methods

4.3.1 Tissue collection

Cancer tissues from the right ovary and omental sites were collected from a woman with stage IIIc, grade 2/3 serous adenocarcinoma at Northside Hospital (Atlanta, GA) after informed consent was obtained under appropriate Georgia Institute of Technology Institutional Review Board protocols (H14337) according to previously described methods performed in accordance with the relevant guidelines and regulations [79]. Briefly, following resection, the tumor tissues were placed in cryotubes and immediately (<1 minute) frozen in liquid nitrogen. Samples were transported on dry ice to Georgia Institute of Technology (Atlanta, GA), and stored at -80 ºC. After examination and verification by

a pathologist, tissues were embedded in cryomatrix (Shandon, ThermoFisher, Waltham, MA). For each tissue sample, 8μm frozen sections were cut and attached to uncharged microscope slides. Following dehydration and staining (HistoGene, LCM Frozen Section Staining Kit, Arcturus, ThermoFisher), slides were processed in an Autopix (Arcturus) instrument for laser capture microdissection (LCM). CapSure Macro-LCM Caps (Arcturus) were used to ensure purity of all collected cells. Approximately 30,000 cells were collected for each of the tissue samples.

4.3.2 RNA extraction and amplification

RNA extraction and amplification were performed according to previously described methods [79]. miRNAs were isolated from the cells using the miRNeasy Micro KIT (Qiagen, Germantown, MD). The quality and quantity of miRNAs were assessed on the Bioanalyzer RNA Pico Chip (Agilent Technologies, Santa Clara, CA). Labeling of miRNAs was performed with the FlashTag Biotin HSR RNA Labeling Kit (Affymetrix) and hybridized to GeneChip® miRNA 3.0 Array chips (Affymetrix, ThermoFisher).

4.3.3 Microarray analysis

Each individual RNA sample was analyzed both for miRNA and mRNA. miRNA profiling analysis was conducted on the GeneChip® miRNA 3.0 Array (Affymetrix). mRNA transcriptome analysis was analyzed using Gene Chip Human Transcriptome Array U133

2.0 (Affymetrix). In total, six miRNA and mRNA (two individual samples in triplicate) global expression data sets were generated in this study.

Raw miRNA and mRNA expression data were processed using Affymetrix Expression Console (EC) Software Version 1.4. Briefly, raw data probes were normalized using SST-RMA algorithm. The normalized expression values were log2 transformed. Differentially expressed mRNAs or miRNAs were identified through fold change and p-value calculated using two-tail Student t-test.

4.3.4 Tissue homogenization, protein extraction and digestion

The minced tissue samples are dounced with tight dounce homogenizer in ice-cold homogenization buffer containing 0.25 M sucrose, 1 mM EDTA, 10 mM HEPES-NaOH, protease inhibitor mixture (Roche Diagnostics, Indianapolis, IN), pH 7.4 with 40 strokes on ice. The solutions were centrifuged at 1,000 g for 10 minutes at 4 ºC. The supernatant was kept, and the tissue pellets were re-suspended in RIPA buffer containing 100 mM 4-(2-hydroxyethyl)-1-piperazineethanesulfonic acid (HEPES), pH=7.9, 150 mM NaCl, 0.5 % sodium dodecyl sulfate (SDS), benzonase (1 U/mL), and protease inhibitor mixture (Roche Diagnostics). After complete solubilization of nuclei and digestion of genomic DNA, the lysate was centrifuged at 25,000 *g* for 10 minutes at 4 ºC. The supernatants were combined, and proteins were reduced by 5 mM DTT (56 °C, 25 min) and alkylated with 15 mM iodoacetamide (RT, 30 minutes in the dark). Proteins were purified with the chloroform-methanol precipitation method. Purified proteins were digested with Lys-C (the ratio of Lys-C and protein was about 1:50) at 31ºC for 15 hours followed by trypsin

digestion at 37 ºC for 4 hours. Digestion was quenched by the addition of 10% TFA to a final concentration of 0.4%, and the resulting peptides were purified using a Sep-Pak tC18 cartridge (Waters, Milford, MA).

4.3.5 Peptide TMT labelling, fractionation and LC-MS/MS analysis

Purified and dried peptides from each sample were tagged with TMT reagents. Each sample was labeled using two channels (*i.e*. the peptides from the tumor tissue of the right ovary were labeled with channel 126 and 127 and the peptides of tumor tissue taken from the omentum were with 128 and 129). The four labeled peptide samples were combined and desalted using a tC18 Sep-Pak cartridge. Then peptides were fractionated using high-pH reversed phase high performance liquid chromatography (HPLC) (pH=10). The sample was fractionated into 20 fractions. Each fraction was purified, dried and dissolved in a solvent containing 5% ACN and 4% formic acid (FA), and 4 µL was loaded onto a microcapillary column packed with C18 beads (Magic C18AQ, 5 µm, 200 Å, 100 µm x 16 cm) using a WPS-3000TPLRS autosampler (Dionex, Sunnyvale, CA). Peptides were separated by reversed-phase chromatography and detected in a hybrid dual-cell quadrupole linear ion trap – Orbitrap mass spectrometer (LTQ Orbitrap Elite, ThermoFisher) using a data-dependent Top 15 method. For each cycle, one full MS scan (resolution: 60,000) in the Orbitrap at 10^6 AGC target was followed by up to 15 MS/MS for the most intense ions. Selected ions were excluded from further analysis for 90 s each. Ions with at least double charges were sequenced. MS/MS scans were activated by HCD at 40.0% normalized collision energy with 1.2 m/z isolation width and detected in the orbitrap cell.

4.3.6 Database searching, data filtering, and quantification

The raw files recorded by MS were converted into mzXML format. Precursors for MS/MS fragmentation were checked for incorrect monoisotopic peak assignments [85]. All MS/MS spectra were matched against a database encompassing sequences of all proteins in the Uniprot Human (*Homo sapiens*) database and common contaminants such as keratins using the SEQUEST algorithm (version 28) [86]. Each protein sequence was listed in both forward and reversed orientations to control and estimate the false discovery rate (FDR) of peptide identifications. The following parameters were used for the database search: 10 ppm precursor mass tolerance; 0.1 Da product ion mass tolerance; full trypsin digestion; up to two missed cleavages; variable modifications: oxidation of methionine (+15.9949); fixed modifications: carbamidomethylation of cysteine (+57.0214), N-terminus and lysine TMT modification (+229.1629).

The target-decoy method was employed to evaluate and further control FDRs of peptide identification [87, 88], and linear discriminant analysis (LDA) was utilized to distinguish correct and incorrect peptide identifications based on multiple parameters such as XCorr, ΔCn, and precursor mass error [85, 89-91]. After scoring, peptides less than six amino acid residues were deleted and peptide spectral matches were filtered to a less than 1% FDR based on the number of decoy sequences in the final data set, then the data set was further filtered to <1% FDR at the protein level.

Quantification of confidently identified peptides was based on the TMT reporter ion intensities in MS [92]. The isotopic information provided by the company (ThermoFisher) was used to calibrate the measured intensities. The median intensity ratio

for each unique peptide in each channel was obtained, and eventually the protein ratio is the median value of all unique peptides for the corresponding protein.

4.3.7 Integration of transcriptomic and proteomic profiles

4436 genes detected by mass spectrometry (FDR<0.01) were mapped to at least one probe set on the HTA 2.0 array by coding gene name matching. For genes with multiple mRNA probes corresponding to a single protein, the probe with the highest average expression level among OV and OM samples was used in the integrated dataset [93].

4.3.8 miRNA target prediction

The miRNA target prediction (based on mirSVR) was downloaded from microRNA.org (August 2010 release) [59]. The mirSVR score refers to targets of microRNAs with scores obtained from their support vector regression algorithm [94]. To reduce the occurrence of false positives, only predicted targets with a mirSVR score less than -0.1 were considered.

4.3.9 Pathway enrichment analysis

Differentially expressed genes on mRNA and protein levels were employed for enrichment analysis using the MetaCore suite 6.29 build 68,613 (Thomson Reuters, New York, NY). Briefly, significantly perturbed pathways and process networks were identified by mapping differentially expressed genes onto manually curated GeneGO canonical pathway maps

and cell process network models [95]. The statistical significance of enrichment was evaluated using p-values calculated based on hypergeometric distribution. Pathways were considered to be significantly enriched if their p-values were < 0.05.

4.3.10 Cell culture and microRNA transfection

The HEY cell line was kindly provided by Gordon Mills, Department of Molecular Therapeutics, University of Texas, MD Anderson Cancer Center. Cells were cultured in RPMI 1640 (Mediatech, Manassas, VA) supplemented with 10% FBS (Fetal Bovine Serum; Atlanta Biologicals, Lawrenceville, GA) and 1% antibiotic-antimycotic solution (Mediatech). For miRNA transfections, 6×10^4 cells were seeded per well in 24-well plates. Cells at exponential phase of growth were transfected with 30 nM miRNA purchased as Pre-miR miRNA Precursors (Ambion, Austin, TX) using Lipofectamine 2000 (Invitrogen, Carlsbad, CA) and per the manufacturer's instructions. Cells were allowed to grow for 48 hours before RNA isolation. Ambion Pre-miR miRNA Precursor Negative Control was used as a negative control.

4.3.11 Real-time PCR

Total RNA was extracted from cells using the RNeasy Mini Kit (Qiagen). Four micrograms of RNA was reversed transcribed into cDNA using the Superscript III First-Strand Synthesis System (Life Technologies, ThermoFisher) according to the manufacturer's instructions. Real-time PCR was performed using TaqMan® Real-Time PCR Master

Mixes (Applied Biosystems, ThermoFisher) on a CFX96 Real-Time System (Bio-Rad, Hercules, CA). Expression values were normalized using *GAPDH* as a reference gene. Normalization and fold-change were calculated using the $\Delta\Delta C_t$ method.

4.3.12 Western Blot

The total protein concentration of the supernatant was determined using a protein assay reagent kit (Bio-Rad). To the lysates, equal volumes of 2X Laemmli sample buffer were added and the samples were heated to 90 °C for 5 minutes. Equal amounts of proteins were separated by 4–20% gradient precast TGX gel (Bio-Rad) and transferred to nitrocellulose membrane (Bio-Rad). Membranes were blocked with 5% nonfat dry milk in 10 mM Tris buffered saline. After blocking, the membranes were probed with the primary antibody for overnight at 4°C with gentle rocking. Antibodies used are against cathepsin B (CTSB antibody Cat # 365558, 1:100 dilutions; Santa Cruz Biotechnologies, Dallas, TX), I-Plastin (PLS1 antibody Cat # 386830, 1:200 dilutions; Santa Cruz Biotechnologies), and Glyceraldehyde-3-phosphate dehydrogenase (GAPDH antibody Cat # 47724, 1:100 dilutions; Santa Cruz Biotechnologies). Appropriate secondary antibodies were used at 1:5,000 dilutions (Santa Cruz Biotechnologies). After incubation with specific horseradish peroxidase–conjugated secondary antibody (goat anti-mouse horseradish peroxidase–(HRP) conjugated secondary antibody (sc-2005, Santa Cruz Biotechnologies), donkey anti-goat horseradish peroxidase–(HRP) conjugated secondary antibody (sc-2020, Santa Cruz Biotechnologies), protein was visualized using the enhanced chemiluminescence

detection system (Pierce, ThermoFisher). The quantification of western blot bands was performed using ImageQuant software (GE Healthcare, Chicago, IL).

4.3.13 Data availability

The microarray datasets supporting the conclusions of this article are available in the Gene Expression Omnibus (GEO) repository, (https://www.ncbi.nlm.nih.gov/geo/query/acc.cgi?acc=GSM947309).

4.4 Results

4.4.1 The majority of changes in gene expression between tumor samples collected from the ovary and omentum of the same patient occur at the post-transcriptional level.

To systematically explore the relationship between RNA and protein expression, we integrated quantitative transcriptional and proteomic profiles of cancer cells isolated by laser capture microdissection from bulk tumor samples collected from the ovary (OV) and the omentum (OM) of the same patient. Expression of mRNA was measured by microarray (Affymetrix Human Transcriptome Array 2.0) as previously described [79]. Protein expression was measured using a recently developed, highly sensitive mass spectrophotometric method [96].

Of the 18,643 genes displaying detectable levels of RNA (Table C.1), the expression of only 4436 were detectable on the protein level (FDR<0.01; Table C.2). The

overall correlation between changes in levels of mRNA and protein encoded by these 4436 genes between the OV and OM samples was low (r=0.38) (Figure 4.1 A), in part, because the majority of the genes displayed little or no change in expression between the OV and OM samples. Of the 4436 genes detected in both our mRNA and protein expression datasets (Figure 4.2; Table C.3), the majority (2490 genes) displayed no significant change in expression (< 1.5-fold change) on either the mRNA or protein levels. Of the 1946 genes displaying a significant change (> 1.5-fold) in expression between the OV and OM samples, 230 were significantly differentially expressed on both the mRNA and protein levels, 1467 were significantly differentially expressed on the protein level but not on the RNA level and 249 on the RNA level but not on the protein level. The overall correlation between changes in RNA and protein for the 1946 significantly differentially expressed genes (Figure 4.1 B; $r = 0.41$, $p = 3.376 \times 10^{-79}$) is in general agreement with similar comparative studies previously carried out on a variety of mammalian tissues, tumors and/or cell lines [82-84, 97-99]. This overall correlation is not greatly affected by increasing the stringency of the cut-off value used in the analysis (Table 4.1).

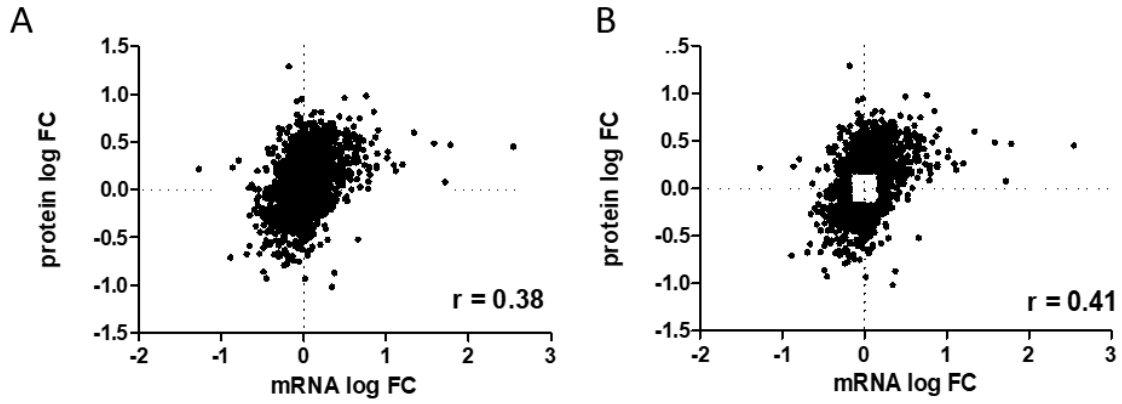

Figure 4.1. Correlation between changes in RNA and protein. Scatterplots with associated correlation coefficients(r) for (A) genes detected in both our mRNA and protein expression datasets (n=4436); (B) genes displaying a significant (p=3.376×10-79) change in expression between the OV and OM samples (n=1946).

Table 4.1. Effects of fold change cut off on Pearson correlation coefficient of differentially expressed genes on mRNA and protein levels.

Fold change	r	p-value
1.2	0.39	2.5E-121
1.5	0.41	3.38E-79
1.8	0.40	8.62E-49
2	0.40	2.38E-35
2.2	0.38	5.29E-26
2.5	0.37	1.28E-17

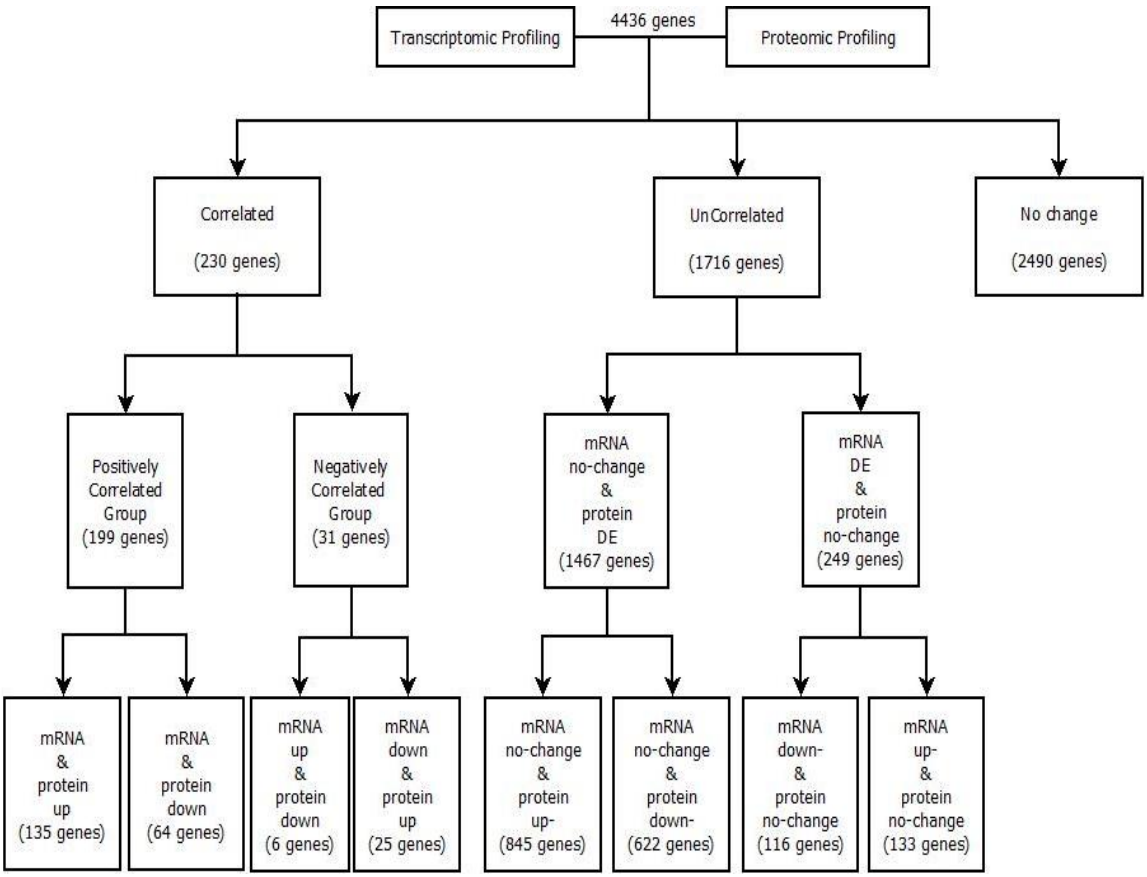

Figure 4.2. Diagram representing the classification of the integrated transcriptomic and proteomic datasets. Step 1: Integration of transcriptomic and proteomic profiling based on gene symbol matching. Step 2: Classification of differentially expressed genes into groups based upon changes in their respective mRNA and protein levels in OV and OM samples.

We further classified genes differentially expressed between the OV and OM samples into three groups based upon changes in their respective mRNA and protein levels: The *positively correlated (PC) group* is comprised of genes displaying positively correlated changes in mRNA and protein levels between the OV and OM samples [*i.e.*, up (mRNA)-up (protein) (U-U); down-down (D-D)]; the *negatively correlated (NC) group* is comprised of genes displaying negatively correlated changes in mRNA and protein levels between the

OV and OM samples [*i.e.*, up (mRNA)-down (protein) (U-D); down-up (D-U)]; and the *uncorrelated (UC) group* is comprised of genes displaying significant changes in the expression of either protein or mRNA levels but not both [*i.e.*, up (mRNA)-no change (protein) (U-NC); no change-up (NC-U); down-no change (D-NC); no change-down (NC-D)]. As shown in Figure 4.3 A, the combined percentage of genes displaying uncorrelated changes (NC-D, NC-U, D-NC, and U-NC) in mRNA and protein levels between the OV and OM samples (88%) far exceeds the percentage of genes (12%) displaying correlated changes. This suggests that the vast majority of changes in gene expression between the OV and OM samples involve processes occurring on the post-transcriptional/translational level. As shown in Figure 4.3 B, most of the uncorrelated changes are in the NC-U sub-group (43%) followed by the NC-D sub-group (32%), the U-NC (7%) and D-NC (6%) sub-groups. Most of the positively correlated changes are in the U-U subgroup (135/199 = 68%) with only 32% (64/199) of the positively correlated changes being in the D-D subgroup. The relatively few changes (1.3%) comprising the negatively correlated group are contained predominantly in the D-U subgroup (25 genes) with only six genes being in the U-D subgroup.

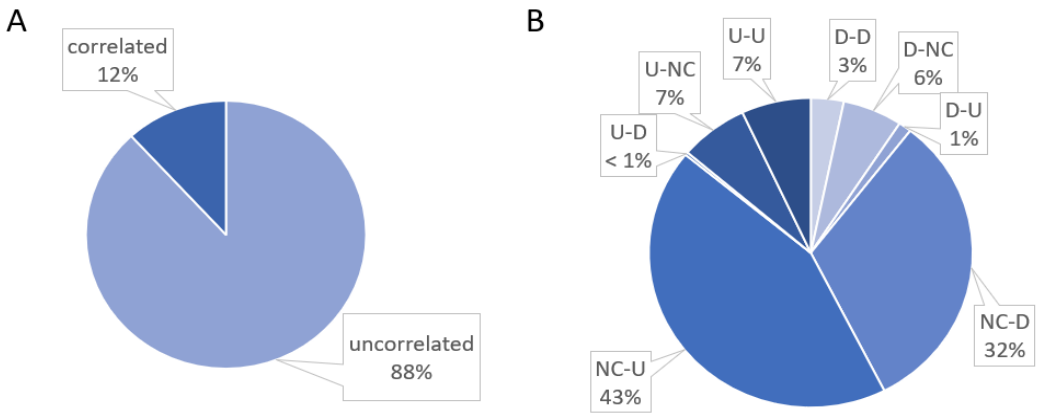

Figure 4.3. Pie chart showing the distribution of genes in correlated and uncorrelated groups. (A) The combined percentage of genes displaying correlated changes (U-U, D-D, D-U, and U-D) and uncorrelated changes (NC-D, NC-U, D-NC, and U-NC) in mRNA and protein levels between the OV and OM. (B) The percentage of genes in each subgroup of correlated and uncorrelated changes.

4.4.2 Gene ontology analyses implicates EMT in the differences observed between samples and underscores the limitations of predictions drawn from RNA profiling alone.

In an effort to evaluate the potential functional significance of the observed changes in RNA and protein expression between the OV and OM samples, we employed gene ontology analyses to compare biological pathways enriched for genes identified as significantly differentially expressed on the RNA and protein levels. Using the combined RNA and protein datasets (1946 genes), a total of 250 biological pathways were identified as being significantly ($p < 0.05$) enriched among genes differentially expressed between the OV and OM samples. Using the RNA expression dataset alone, 73 pathways were identified as being significantly enriched, while 218 were significantly enriched using the

protein dataset alone (Table C.4, Table C.5). There was an overlap of only 41 biological pathways (16%) enriched in the two datasets (Figure 4.4 A, 4.4 B). More than half of the 41 overlapping biological pathways uncovered in our analysis (*e.g.*, cell adhesion and cytoskeleton remodeling, *etc*.) are either directly or indirectly associated with epithelial-to-mesenchymal transition (EMT)- a cellular function believed to be critical in cancer metastasis [100, 101].

While the 41 overlapping pathways constitute the majority of those predicted from the RNA dataset alone (41/73 = 56%), nearly half of the pathways predicted to be significantly overrepresented from the RNA dataset are likely spurious since these RNA changes are not manifest on the protein level. This finding coupled with the fact that >80% (177/218) of the pathways predicted from the protein dataset were not predicted from the RNA dataset points to the limitations of functional pathway predictions drawn from RNA profiling alone.

The fact that many pathways known to be central to EMT and other aspects of metastasis were significantly enriched among genes differentially expressed on the protein but not the RNA level (*e.g.*, development-TGF-beta-dependent induction of EMT via MAPK, cell adhesion-role of tetraspanins in the integrin-mediated cell adhesion, cytoskeleton remodeling-Fibronectin-binding integrins in cell motility, *etc*.) further supports the functional importance of post-transcriptional/translational regulatory controls and underscores the importance of understanding the molecular mechanisms involved.

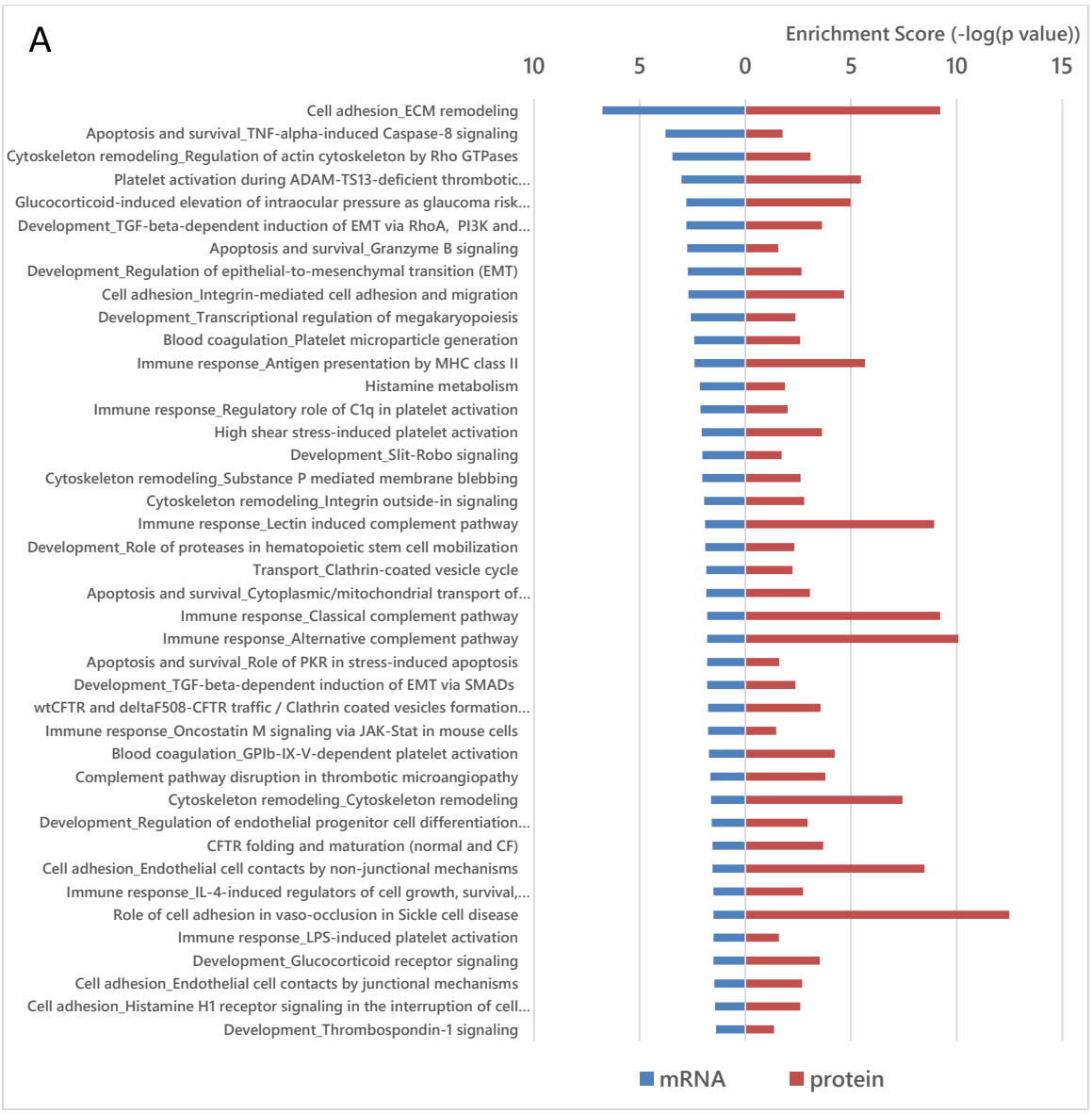

Figure 4.4. Results of GeneGo pathway enrichment analysis. (A) 41 GeneGo pathways significantly enriched in differentially expressed genes on either mRNA or protein

level. (p-value < 0.05) (B) Venn diagram shows the number of enriched GeneGo pathways of each dataset that were found to be significantly enriched. (p-value < 0.05)

4.4.3 Differences in microRNA (miRNA) expression contribute to post-transcriptional/translational changes between the OV and OM samples.

The discordance between changes in levels of protein and their encoding mRNAs can be explained in a variety of ways including differences in relative rates of *in vivo* synthesis and stability [102]. While some differences in RNA/protein stability can be attributed to inherent differences in molecular structure, emerging evidence suggests that relative rates of both protein synthesis and RNA/protein stability are often post-transcriptionally regulated by microRNAs (miRNAs) [103].

MiRNAs are small, non-encoding regulatory RNAs that can post-transcriptionally regulate levels of RNA and protein by degrading targeted mRNAs and/or by repressing translation of targeted mRNA transcripts [104]. To explore the possible role of miRNAs in the observed discordance between mRNA and protein levels between the OV and OM samples, we measured changes in levels of miRNAs and correlated these changes with corresponding changes in levels of mRNA and protein of their targeted genes. Differences in levels of miRNAs between the OV and OM samples were determined by microarray (Affymetrix GeneChip® miRNA 3.0 Array) and the mRNAs targeted by the differentially expressed miRNAs predicted using the miRanda-mirSVR algorithm [94]. Our focus was on genes displaying significant decreases in protein levels in the OM sample with no corresponding change in levels of mRNA (NC-D group). Our goal was to test the

hypothesis that at least some of the observed discordance might be explained by the up-regulation of regulatory miRNAs.

The NC-D group is comprised of 622 genes, 592 of which are predicted to be targeted by 1100 miRNAs (Table C.6). Of these 1100 miRNAs, 101 are significantly differentially expressed between the OV and OM samples (Table C.7) and 48 of these are significantly up regulated in the OM sample (Table C.8). For example, the 10 most significantly up-regulated of these miRNAs and the number of their predicted gene targets in the NC-D and D-D groups is shown in Table 1. Interestingly, the gene targets of miRNAs significantly up regulated in the OM sample are contained in both the D-D and NC-D groups (Table C.9, Table C.10). This implies that individual miRNAs up regulated in the OM sample may be regulating some genes on the transcriptional level (effecting down regulation of mRNAs and correlated changes on the protein level) and some genes on the translational level (effecting levels of protein with no correlated change on the mRNA level).

In an effort to independently validate the observation that single miRNAs may preferentially regulate different genes on different levels (*i.e.*, transciptionally vs. post-transcriptionally), we selected the most significantly up-regulated miRNA in OM, hsa-miR-363-3p, and exogenously over-expressed it in the well-characterized HEY ovarian cancer cell line [105]. Forty-eight hours after transfection of miR-363-3p in HEY cells, we extracted mRNA and protein, and monitored levels of two randomly selected genes, one from the D-D group (*CTSB*, Cathepsin B) and one from the NC-D group (*PLS1*, Plastin1). Western blots demonstrate that levels of CTSB and PLS1 protein are both decreased in cells in which hsa-miR-363-3p was over expressed (Figure 4.5 A, 4.5 C). RT-PCR

quantification of mRNA levels of these two genes showed a significant decrease in CTSB mRNA levels but no significant change in levels of PLS1 mRNA (Figure 4.5 B). The results of this experiment are consistent with the results of our RNA microarray and protein mass spectrometric analyses indicating that changes in levels of the same miRNAs may alternatively regulate levels of RNA and/or proteins in a gene-specific manner.

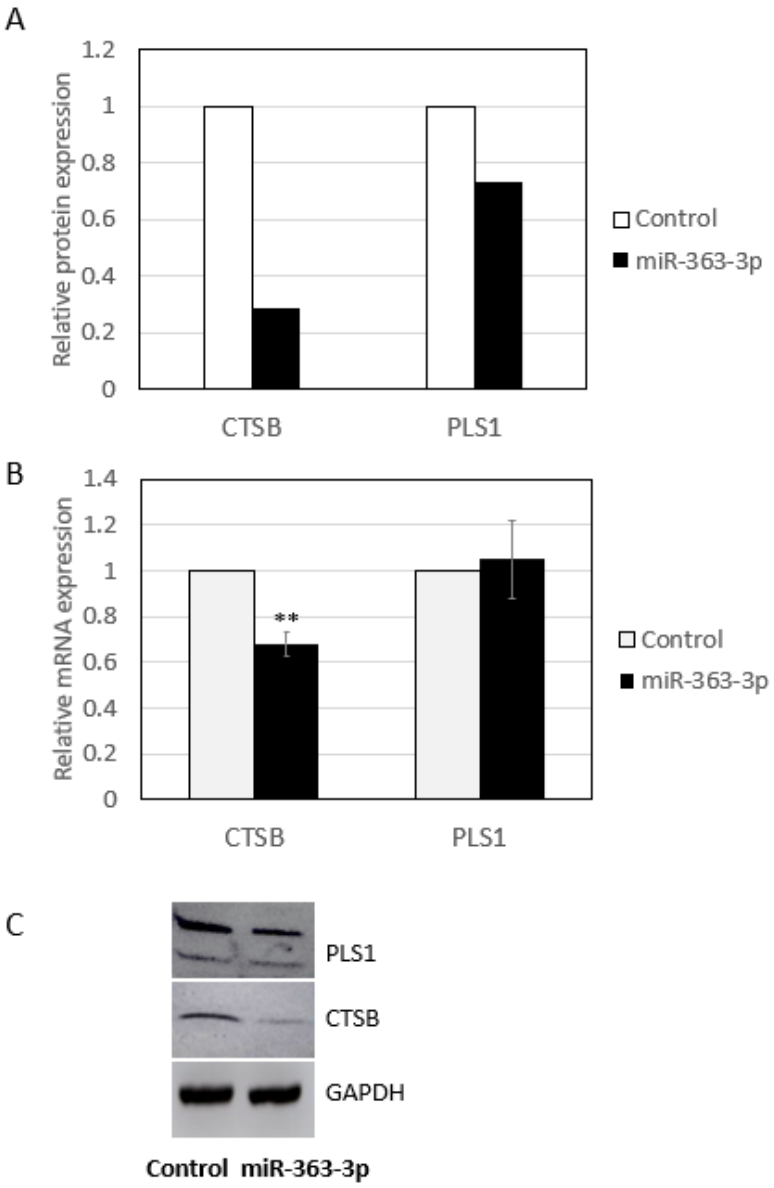

Figure 4.5. Effects of over-expression of miR-363-3p in HEY cells on the mRNA and protein expression of its predicted targets CTSB and PLS1. (A) Relative protein expression levels of CTSB and PLS1 as determined by Western blot. (B) Relative mRNA expression of CTSB and PLS1 as determined by qRT-PCR shows a significant decrease in CTSB mRNA levels but no significant changes on levels of PLS1. Expression values are normalized to negative control group and represent mean ± SD of at least three biological replicates each performed in three technical replicates. Asterisks represent statistically significant differences from the negative control group. (: $p<0.05$) (C) Western blot analysis of CTSB and PLS1 proteins both display reduced levels of protein in the miR-363-3p group relative to negative control group.**

4.5 Discussion

Modern DNA sequencing methods can identify genetic differences in cancer vs. normal tissues with nucleotide precision. Similarly, microarray, RNA sequencing and related high-throughput methodologies can quantitate changes in levels of gene expression on the RNA level with remarkable accuracy. The problem is that although the consequences of nearly all genome-wide molecular level changes manifest their functional significance on the protein level, global changes in the levels of protein are not easily and economically monitored by current methods. As a consequence, global changes in protein levels associated with cancer onset and progression are typically not directly measured but rather inferred from more easily monitored changes on the RNA level. The validity of these inferences is often questionable and, in some instance, may be misleading [81, 106]. For example, modern cancer medicine is rapidly embracing the molecular profiling of patient tumors in order to personalize targeted gene therapies [107]. Significant over-expression of a particular "cancer driver" gene on the RNA level may suggest treatment with a chemical inhibitor of the protein encoded by the over-expressed RNA. This may be a reasonable therapeutic strategy but only if elevated levels of mRNAs are an accurate reflection of levels of the targeted proteins.

The purpose of this study was to explore the system-wide relationship between differences in gene expression on the RNA and protein levels between tumor samples collected from the same patient. Using recently developed proteomic methodologies, we were able to explore this question on a global, level by directly comparing the expression of 4436 genes simultaneously on the RNA and protein levels.

We compared system-wide changes in levels of RNA and protein between discrete tumor samples collected from the ovary and the omentum of the same OC patient. Comparing molecular profiles between samples collected from the same patient removes the ambiguities associated with between-patient variation and allowed us to focus on changes associated with tumor progression within a single patient. Our results indicate that the majority of changes in mRNA and protein expression are not correlated with one another, consistent with emerging evidence for the importance of post-transcriptional/translational regulation in various aspects of cancer onset and progression [106].

There remains controversy as to whether OC metastases originate from primary tumors in the fallopian tube, in the ovary or both[24]. While our studies do not resolve this controversy, our gene ontology (GO) analyses indicate that, for the patient analyzed in this study, the majority of biological pathways associated with the RNA and protein level changes between the OV and OM samples are associated with EMT. This is consistent with the growing body of evidence that EMT is critical to the metastatic process [100, 101]. The fact that the majority of changes in biological pathways between the OV and OM samples were predicted from the observed changes in protein and not RNA levels further supports the importance of post-transcriptional regulation in metastasis.

Because of the growing body of evidence implicating miRNAs in various aspects of cancer onset and progression [108], we explored the possibility that miRNAs may be contributing to the observed discordance between changes in RNA and protein levels in our OV and OM samples. We measured changes in levels of miRNAs between OV and OM samples and correlated these changes with corresponding changes in levels of mRNA

and protein of their targeted genes. Our focus was on testing the hypothesis that at least some of the genes displaying significant decreases in protein levels in the OM sample with no corresponding change in levels of mRNA (NC-D group) might be explained by the up regulation of regulatory miRNAs. Consistent with this hypothesis, we found that gene targets of miRNAs significantly up regulated in the OM sample are down regulated on the RNA and or protein levels. In some instances, individual miRNAs up regulated in the OM sample are associated with down regulation of their targeted mRNAs with a correlated down regulation on the protein level. In other instances, the same miRNAs up regulated in the OM sample were associated with significant down regulation of their targeted proteins but no correlated change in levels of their encoding mRNAs indicating a miRNA-mediated regulatory block on the translational level. This suggests that individual miRNAs up regulated in the OM sample may be regulating some genes on the RNA level and other genes on the protein level.

The possibility that a single miRNA may preferentially regulate different genes on different levels (*i.e*., transcriptional vs. translational) was corroborated by *in vitro* studies. Although the extensiveness and mechanisms underlying this phenomenon remains to be determined, previous studies have shown that the association of miRNAs with RNA binding proteins can significantly affect the levels (post-transcriptional and/or translational) on which individual miRNAs regulate their target genes [109].

Collectively, our findings indicate that a significant fraction of the discordance in changes in RNA and protein levels between our samples are mediated by miRNAs and that miRNAs may contribute to the regulatory coordination of changes on the RNA and protein levels to enhance metastasis.

Overall, our findings are consistent with growing evidence of the importance of post-transcriptional/translational changes in the onset and progression of ovarian and other cancers and the potential significance of miRNAs in regulating the process.

CHAPTER 5. CONCLUSIONS

MiRNAs are important transcriptional and post-transcriptional regulators of gene expression. Based on base paring, miRNAs are able to bind to the 3'-UTR of the target genes and typically down-regulate their target gene expression [110]. One miRNA is able to regulate the gene expression of multiple target genes, and one target gene can be regulated by multiple miRNAs [111]. As a result, miRNAs are able to regulate about 60% of the known human genes and are involved in almost every molecular pathway [112]. Recent studies have suggested that dysregulated miRNAs are involved in the hallmarks of cancer, including sustaining proliferative signaling, evading growth suppressors, resisting cell death, activating invasion and metastasis, and inducing angiogenesis [113]. In this thesis, I examine the role of miRNAs in regulating EMT/MET in ovarian cancer.

In the first study (Chapter 2), we show that sequentially divergent miRNAs converge to regulate the EMT/MET process through both direct and indirect regulatory changes. We present evidence that helps explain how sequentially divergent miRNAs (miR-205 and miR-200 family members) are able to induce MET in ovarian cancer HEY cells. We first demonstrated that miR-205 and the miR-200 family of miRNAs both induce MET in mesenchymal-like ovarian cancer cells by affecting both direct and indirect changes in the expression of genes. We next demonstrate that the majority of changes in gene expression commonly induced by ectopic over-expression of the miR-200 family of miRNAs and miR-205 are the result of indirect regulatory controls, specifically in the changes in expression of EMT/MET-associated genes. While only two direct targets of these miRNAs (ZEB1 and WNT5A) are commonly down regulated in response to over

expression of miR-205 and/or the miR-200 family of miRNAs, down regulation of these genes alone or in combination only partially recapitulated the changes induced by the miRNAs. This indicates an auxiliary contribution of other direct and/or indirect regulatory changes induced in common or individually by the miRNAs. We go on to provide evidence that regulation of EMT/MET associated genes by miR-205 is the result of convergent evolution brought about by a translocation event linking miR-205 with members of the miR-200 family on human chromosome 1 approximately 80 MYA.

In the second study (Chapter 3), we explore the impact of genetic difference between different cancer cell lines on the function of miRNAs to regulate the EMT/MET process. We demonstrate that the overexpression of miR-205 induces a morphological change to a more rounded/cuboidal phenotype consistent with MET in the two OC cells (HEY and SKOV3) but not in prostate cancer cells (PC3) relative to negative controls. In contrast, miR-203a induces morphological changes characteristic of MET in PC3 cells but not in the HEY and SKOV3 cells, while miR-429 induces morphological changes characteristics of MET in all three of the cell lines. We report that the ability of these sequentially divergent miRNAs to induce MET in these cells is found to be associated with inherent differences in the starting molecular profiles of the untreated cancer cells, as well as, variability in trans-regulatory controls modulating the expression of genes targeted by the individual miRNAs. Our results help support the view that miRNAs have significant potential as cancer therapeutic agents.

Throughout our first two studies, we focused on the regulatory mechanisms of miRNAs mostly from the transcriptional level; however, miRNAs have been shown to regulate their target gene expression on both the transcriptional and post-transcriptional

levels. In the final study (Chapter 4), we evaluate the importance of post-transcriptional/translational changes in the metastasis of a stage III ovarian cancer patient and the role played by miRNAs in regulating the process. We present evidence that the majority of changes in gene expression between tumor samples collected from the ovary and omentum of the same patient occur at the post-transcriptional level. We first proved that the overall correlation between global changes in levels of mRNAs and their encoding proteins is low ($r=0.38$). We next verified that the majority of differences are on the protein level with no corresponding change on the mRNA level. More importantly, we revealed the limitation of drawing conclusions of functional predictions of the differentially expressed genes from RNA profiling alone. We further validated that a significant fraction of the discordance in changes on the RNA and protein levels between our samples are mediated by miRNAs. Our results provide an example of the contribution of miRNAs in the regulatory coordination of changes on the RNA and protein levels to enhance metastasis.

All three studies, while taking different approaches, emphasize the scope and complexity of miRNA mediated gene expression regulation.

APPENDIX A. SUPPLEMENTARY DATA FOR CHAPTER 2

Table A.1. Gene expression profiles of HEY cells after transfection of miR-NC, miR-141, miR-200b, miR-205 for 48 hours. Gene expression profiles are normalized and log2 transformed using the RMA method.

Table A.2. miRanda predicted target genes of miR-141, miR-200b and miR-205. 3943, 4027, and 2941 genes are predicted to be direct target genes of miR-141, miR-200b, and miR-205, respectively. Among these, 1440 genes are predicted to be direct target genes of both miR-141 and miR-200b, but only 444 out of these 1440 genes (30.8%) are predicted to be direct target genes of miR-205.

Table A.3. TargetScan predicted target genes of miR-141, miR-200b and miR-205. 679, 666, and 508 genes are predicted to be direct target genes of miR-141, miR-200b, and miR-205, respectively. Among these, 99 genes are predicted to be direct target genes of both miR-141 and miR-200b, but only 13 out of these 99 genes (13.1%) are predicted to be direct target genes of miR-205.

Table A.4. miRDB predicted target genes of miR-141, miR-200b and miR-205. 759, 757, and 269 genes are predicted to be direct target genes of miR-141, miR-200b, and miR-205, respectively. Among these, 104 genes are predicted to be direct target genes of both miR-141 and miR-200b, but only 8 out of these 104 genes (7.7%) are predicted to be direct target genes of miR-205.

Table A.5. Gene expression profiles of the 16 gene panel of canonical EMT genetic markers in HEY cells after transfection of si-NC, si-ZEB1, si-WNT5A, or si-ZEB1-WNT5A for 48 hours. Gene expression profiles are normalized and log2 transformed using RMA method.

Table A.6. EMT/MET associated target genes of miR-200 family members (miR-141, miR-200b) and miR-205. miR-141, miR-200b target 20, 28 EMT/MET associated genes, whereas miR-205 targets 18 EMT/MET associated genes.

Table A.7. EMT/MET associated target genes of miR-200 family members (miR-141/200b) and miR-205 in human and mouse. miRNA target predictions of human and mouse were downloaded from microRNA.org. To reduce false positive results, only the predicted targets with mirSVR score < -0.1 were included.

APPENDIX B. SUPPLEMENTARY DATA FOR CHAPTER 3

Table B.1. Gene expression profiles of un-transfected and transfected (miR-NC, miR-203a, miR-205, and miR-429) HEY, SK-OV-3, and PC-3 cells.

Table B.2. miRNA-mediated de-repression of repressor genes overrides expected down-regulatory effects of miRNA in HEY cells.

Table B.3. miRNA-mediated de-repression of repressor genes overrides expected down-regulatory effects of miRNA in SK-OV-3 cells.

Table B.4. miRNA-mediated de-repression of repressor genes overrides expected down-regulatory effects of miRNA in PC-3 cells.

Table B.5. List of 84 genes that have been previously implicated to be important in the regulation of EMT/MET process.

Table B.6. Genes targeted by the over expressed miR-203a that displayed changes in levels of expression consistent with the miRNA-induced changes in morphology and correlated EMT scores.

Table B.7. Genes targeted by the over expressed miR-205 that displayed changes in levels of expression consistent with the miRNA-induced changes in morphology and correlated EMT scores.

Table B.8. Genes targeted by the over expressed miR-429 that displayed changes in levels of expression consistent with the miRNA-induced changes in morphology and correlated EMT scores.

Table B.9. miR-203a and miR-205 target binding site sequence comparison between SK-OV-3 and PC-3 cells.

Table B.10. Expression levels of miR-203a target gene SNAI2 and its known repressor genes.

APPENDIX C. SUPPLEMENTARY DATA FOR CHAPTER 4

Table C.1. Gene Symbol, Probe Set ID, and normalized expression value of the 18,643 genes (19867 probe sets) detected in POC and MOC samples.

Table C.2. Gene Symbol, Uniport Reference Number, protein annotation, and fold change of 4436 genes (4460 isoforms) identified (FDR < 0.01) in POC and MOC samples by mass spectrometry.

Table C.3. Integration of the microarray and mass spec profiles identified 4436 genes found in both datasets.

Table C.4. GeneGO biological pathways significantly enriched ($p < 0.05$) among genes differentially expressed between the POC and MOC samples on mRNA levels.

Table C.5. GeneGO biological pathways significantly enriched ($p < 0.05$) among genes differentially expressed between the POC and MOC samples on protein levels.

Table C.6. miRNAs and their target genes in the NC-D group (FC = 1.5).

Table C.7. Differentially expressed ($p < 0.05$ and $FC > 1.5$) miRNAs and their target genes in the NC-D group.

Table C.8. Up-regulated ($p < 0.05$ and $FC > 1.5$) miRNAs in the MOC sample and their target genes in the NC-D group (FC = 1.5).

Table C.9. Up-regulated ($p < 0.05$ and $FC > 1.5$) miRNAs in the MOC sample and their targets in D-D group (FC = 1.5).

Table C.10. Up-regulated ($p < 0.05$ and $FC > 1.5$) miRNAs in the MOC sample and their targets in the NC-D group (FC = 1.5).

PUBLICATIONS

Zhang, M., Matyunina, L.V., Walker, L.D., Chen, W., Xiao, H., Benigno, B.B., Wu, R., and McDonald, J.F. (2017) Evidence for the importance of post-transcriptional regulatory changes in ovarian cancer progression and the contribution of miRNAs. Scientific Reports. 7:8171.

Zhang, M., Jabbari, N., Satpathy M., Matyunina, L.V., Wang, Y., McDonald, L.D., McDonald, J.F. Sequentially divergent miRNAs converge to induce mesenchymal-to-epithelial transition in ovarian cancer cells through direct and indirect regulatory controls. Cancer Letters. *Under Review*.

Lili LN, Huang AD, **Zhang M**, Wang L, McDonald LD, Matyunina LV, Satpathy M, McDonald JF. 2018. Time-course analysis of microRNA-induced mesenchymal-to-epithelial transition underscores the complexity of the underlying molecular processes. Cancer Letters, 2018. 428: p. 184-191.

Elliott, B., A. C. Millena, L. Matyunina, **M. Zhang**, J. Zou, G. Wang, Q. Zhang, N. Bowen, V. Eaton, G. Webb, S. Thompson, J. McDonald and S. Khan (2019). Essential role of JunD in cell proliferation is mediated via MYC signaling in prostate cancer cells. Cancer Letters. 2019. 448: p. 155-167

REFERENCES

1. Majeti, R., et al., *Dysregulated gene expression networks in human acute myelogenous leukemia stem cells.* Proceedings of the National Academy of Sciences, 2009. **106**(9): p. 3396-3401.

2. Wang, J., Q. Liu, and Y. Shyr, *Dysregulated transcription across diverse cancer types reveals the importance of RNA-binding protein in carcinogenesis.* BMC Genomics, 2015. **16**(7): p. S5.

3. Zhang, F. and D. Wang, *The Pattern of microRNA Binding Site Distribution.* Genes (Basel), 2017. **8**(11).

4. Price, C. and J. Chen, *MicroRNAs in Cancer Biology and Therapy: Current Status and Perspectives.* Genes & diseases, 2014. **1**(1): p. 53-63.

5. Lu, J., et al., *MicroRNA expression profiles classify human cancers.* Nature, 2005. **435**(7043): p. 834-8.

6. Mongroo, P.S. and A.K. Rustgi, *The role of the miR-200 family in epithelial-mesenchymal transition.* Cancer biology & therapy, 2010. **10**(3): p. 219-222.

7. Jabbari, N., A.N. Reavis, and J.F. McDonald, *Sequence variation among members of the miR-200 microRNA family is correlated with variation in the ability to induce hallmarks of mesenchymal-epithelial transition in ovarian cancer cells.* Journal of ovarian research, 2014. **7**: p. 12-12.

8. Gregory, P.A., et al., *The miR-200 family and miR-205 regulate epithelial to mesenchymal transition by targeting ZEB1 and SIP1.* Nature Cell Biology, 2008. **10**: p. 593.

9. Hill, C.G., et al., *Functional and evolutionary significance of human microRNA seed region mutations.* PLoS One, 2014. **9**(12): p. e115241.

10. Jackson, R.J. and N. Standart, *How do microRNAs regulate gene expression?* Sci STKE, 2007. **2007**(367): p. re1.

11. Weigelt, B., J.L. Peterse, and L.J. van 't Veer, *Breast cancer metastasis: markers and models.* Nat Rev Cancer, 2005. **5**(8): p. 591-602.

12. Lambert, A.W., D.R. Pattabiraman, and R.A. Weinberg, *Emerging Biological Principles of Metastasis.* Cell, 2017. **168**(4): p. 670-691.

13. Fidler, I.J., *The pathogenesis of cancer metastasis: the 'seed and soil' hypothesis revisited.* Nature Reviews Cancer, 2003. **3**: p. 453.

14. Thiery, J.P., *Epithelial–mesenchymal transitions in tumour progression.* Nature Reviews Cancer, 2002. **2**: p. 442.

15. Nieto, M.A., et al., *EMT: 2016.* Cell, 2016. **166**(1): p. 21-45.

16. Mehlen, P. and A. Puisieux, *Metastasis: a question of life or death.* Nat Rev Cancer, 2006. **6**(6): p. 449-58.

17. Evdokimova, V., et al., *Reduced proliferation and enhanced migration: two sides of the same coin? Molecular mechanisms of metastatic progression by YB-1.* Cell Cycle, 2009. **8**(18): p. 2901-6.

18. Patel, P. and E.I. Chen, *Cancer stem cells, tumor dormancy, and metastasis.* Frontiers in endocrinology, 2012. **3**: p. 125-125.

19. Chaffer, C.L. and R.A. Weinberg, *A Perspective on Cancer Cell Metastasis.* Science, 2011. **331**(6024): p. 1559-1564.

20. Guo, F., et al., *Post-transcriptional regulatory network of epithelial-to-mesenchymal and mesenchymal-to-epithelial transitions.* Journal of Hematology & Oncology, 2014. **7**(1): p. 19.

21. Burger, G.A., E.H.J. Danen, and J.B. Beltman, *Deciphering Epithelial-Mesenchymal Transition Regulatory Networks in Cancer through Computational Approaches.* Frontiers in oncology, 2017. **7**: p. 162-162.

22. Wendt, M.K., T.M. Allington, and W.P. Schiemann, *Mechanisms of the epithelial-mesenchymal transition by TGF-beta.* Future oncology (London, England), 2009. **5**(8): p. 1145-1168.

23. Fantozzi, A., et al., *VEGF-mediated angiogenesis links EMT-induced cancer stemness to tumor initiation.* Cancer Res, 2014. **74**(5): p. 1566-75.

24. Gasior, K., et al., *A Theoretical Model of the Wnt Signaling Pathway in the Epithelial Mesenchymal Transition.* Theor Biol Med Model, 2017. **14**(1): p. 19.

25. Wang, Z., et al., *The role of Notch signaling pathway in epithelial-mesenchymal transition (EMT) during development and tumor aggressiveness.* Current drug targets, 2010. **11**(6): p. 745-751.

26. Goossens, S., et al., *EMT transcription factors in cancer development re-evaluated: Beyond EMT and MET.* Biochim Biophys Acta Rev Cancer, 2017. **1868**(2): p. 584-591.

27. Kahlert, U.D., J.V. Joseph, and F.A.E. Kruyt, *EMT- and MET-related processes in nonepithelial tumors: importance for disease progression, prognosis, and therapeutic opportunities.* Mol Oncol, 2017. **11**(7): p. 860-877.

28. Yang, J., et al., *Integrated proteomics and genomics analysis reveals a novel mesenchymal to epithelial reverting transition in leiomyosarcoma through regulation of slug.* Molecular & cellular proteomics : MCP, 2010. **9**(11): p. 2405-2413.

29. Xu, Q., et al., *Long non-coding RNA regulation of epithelial-mesenchymal transition in cancer metastasis.* Cell death & disease, 2016. **7**(6): p. e2254-e2254.

30. Cursons, J., et al., *Combinatorial Targeting by MicroRNAs Co-ordinates Post-transcriptional Control of EMT.* Cell Syst, 2018. **7**(1): p. 77-91.e7.

31. Abba, M.L., et al., *MicroRNA Regulation of Epithelial to Mesenchymal Transition.* Journal of clinical medicine, 2016. **5**(1): p. 8.

32. Kozomara, A., M. Birgaoanu, and S. Griffiths-Jones, *miRBase: from microRNA sequences to function.* Nucleic Acids Res, 2019. **47**(D1): p. D155-d162.

33. Ha, M. and V.N. Kim, *Regulation of microRNA biogenesis.* Nature Reviews Molecular Cell Biology, 2014. **15**: p. 509.

34. Lewis, B.P., et al., *Prediction of mammalian microRNA targets.* Cell, 2003. **115**(7): p. 787-98.

35. Friedman, R.C., et al., *Most mammalian mRNAs are conserved targets of microRNAs.* Genome Res, 2009. **19**(1): p. 92-105.

36. Pasquinelli, A.E., *Paring MiRNAs Through Pairing.* Science, 2010. **328**(5985): p. 1494-1495.

37. Park, S.-M., et al., *The miR-200 family determines the epithelial phenotype of cancer cells by targeting the E-cadherin repressors ZEB1 and ZEB2.* Genes & development, 2008. **22**(7): p. 894-907.

38. Tseng, J.H., et al., *miR-200c-driven Mesenchymal-To-Epithelial Transition is a Therapeutic Target in Uterine Carcinosarcomas.* Scientific Reports, 2017. **7**(1): p. 3614.

39. Larzabal, L., et al., *TMPRSS4 regulates levels of integrin α5 in NSCLC through miR-205 activity to promote metastasis.* British Journal of Cancer, 2014. **110**(3): p. 764-774.

40. Gandellini, P., et al., *miR-205 Exerts Tumor-Suppressive Functions in Human Prostate through Down-regulation of Protein Kinase Cε.* Cancer Research, 2009. **69**(6): p. 2287-2295.

41. Wang, L., et al., *Ectopic over-expression of miR-429 induces mesenchymal-to-epithelial transition (MET) and increased drug sensitivity in metastasizing ovarian cancer cells.* Gynecol Oncol, 2014. **134**(1): p. 96-103.

42. Macedo, T., et al., *Overexpression of mir-183 and mir-494 promotes proliferation and migration in human breast cancer cell lines.* Oncol Lett, 2017. **14**(1): p. 1054-1060.

43. Song, X., et al., *MicroRNA-492 overexpression exerts suppressive effects on the progression of osteosarcoma by targeting PAK7.* Int J Mol Med, 2017. **40**(3): p. 891-897.

44. Lee, C.G., et al., *MicroRNA-147 induces a mesenchymal-to-epithelial transition (MET) and reverses EGFR inhibitor resistance.* PLoS One, 2014. **9**(1): p. e84597.

45. Jabbari, N., A.N. Reavis, and J.F. McDonald, *Sequence variation among members of the miR-200 microRNA family is correlated with variation in the ability to induce hallmarks of mesenchymal-epithelial transition in ovarian cancer cells.* J Ovarian Res, 2014. **7**: p. 12.

46. Viticchie, G., et al., *MiR-203 controls proliferation, migration and invasive potential of prostate cancer cell lines.* Cell Cycle, 2011. **10**(7): p. 1121-31.

47. Leavitt, S.A., *"Deciphering the Genetic Code: Marshall Nirenberg".* Office of NIH History., 2010.

48. Maier, T., M. Güell, and L. Serrano, *Correlation of mRNA and protein in complex biological samples.* FEBS Letters, 2009. **583**(24): p. 3966-3973.

49. McManus, J., Z. Cheng, and C. Vogel, *Next-generation analysis of gene expression regulation--comparing the roles of synthesis and degradation.* Mol Biosyst, 2015. **11**(10): p. 2680-9.

50. Uhlén, M., et al., *Tissue-based map of the human proteome.* Science, 2015. **347**(6220): p. 1260419.

51. Peshkin, L., et al., *On the Relationship of Protein and mRNA Dynamics in Vertebrate Embryonic Development.* Developmental Cell, 2015. **35**(3): p. 383-394.

52. Cannell, I.G., Y.W. Kong, and M. Bushell, *How do microRNAs regulate gene expression?* Biochem Soc Trans, 2008. **36**(Pt 6): p. 1224-31.

53. Lamouille, S., J. Xu, and R. Derynck, *Molecular mechanisms of epithelial–mesenchymal transition.* Nature reviews. Molecular cell biology, 2014. **15**(3): p. 178-196.

54. Zhang, J. and L. Ma, *MicroRNA control of epithelial–mesenchymal transition and metastasis.* Cancer metastasis reviews, 2012. **31**(0): p. 653-662.

55. Li, W.-H.W., Chung-I; Luo, Chi-Cheng., *A New Method for Estimating Synonymous and Nonsynonymous Rates of Nucleotide Substitution Considering the*

Relative Likelihood of Nucleotide and Codon Changes., in *Molecular Biology and Revolution*. 1985. p. 150-174.

56. Zhang, M., et al., *Evidence for the importance of post-transcriptional regulatory changes in ovarian cancer progression and the contribution of miRNAs.* Scientific Reports, 2017. **7**(1): p. 8171.

57. Ritchie, M.E., et al., *limma powers differential expression analyses for RNA-sequencing and microarray studies.* Nucleic Acids Res, 2015. **43**(7): p. e47.

58. Hill, C.G., et al., *Functional and evolutionary significance of human microRNA seed region mutations.* PloS one, 2014. **9**(12): p. e115241-e115241.

59. Betel, D., et al., *The microRNA.org resource: targets and expression.* Nucleic Acids Res, 2008. **36**(Database issue): p. D149-53.

60. Wong, N. and X. Wang, *miRDB: an online resource for microRNA target prediction and functional annotations.* Nucleic Acids Res, 2015. **43**(Database issue): p. D146-52.

61. Agarwal, V., et al., *Predicting effective microRNA target sites in mammalian mRNAs.* Elife, 2015. **4**.

62. Carpenter, A.E., et al., *CellProfiler: image analysis software for identifying and quantifying cell phenotypes.* Genome Biol, 2006. **7**(10): p. R100.

63. Chen, J., et al., *Overexpression of miR-429 induces mesenchymal-to-epithelial transition (MET) in metastatic ovarian cancer cells.* Gynecol Oncol, 2011. **121**(1): p. 200-5.

64. Lili, L.N., et al., *Time-course analysis of microRNA-induced mesenchymal-to-epithelial transition underscores the complexity of the underlying molecular processes.* Cancer Lett, 2018. **428**: p. 184-191.

65. Shahab, S.W., et al., *The effects of MicroRNA transfections on global patterns of gene expression in ovarian cancer cells are functionally coordinated.* BMC medical genomics, 2012. **5**: p. 33-33.

66. https://www.qiagen.com/us/shop/pcr/primer-sets/rt2-profiler-pcr-arrays/?catno=PAHS-090Z#geneglob.

67. Gibbons, D.L. and C.J. Creighton, *Pan-cancer survey of epithelial-mesenchymal transition markers across the Cancer Genome Atlas.* Dev Dyn, 2018. **247**(3): p. 555-564.

68. Hasuwa, H., et al., *MiR-200b and miR-429 Function in Mouse Ovulation and Are Essential for Female Fertility.* Science, 2013. **341**(6141): p. 71-73.

69. Shin, J.-O., et al., *miR-200b regulates cell migration via Zeb family during mouse palate development.* Histochemistry and Cell Biology, 2012. **137**(4): p. 459-470.

70. van Oers, N.S., et al., *MIR205HG is a Long Noncoding RNA with Distinct Functions in the Thymus versus the Anterior Pituitary.* The Journal of Immunology, 2018. **200**(1 Supplement): p. 165.11-165.11.

71. Wiklund, E.D., et al., *Coordinated epigenetic repression of the miR-200 family and miR-205 in invasive bladder cancer.* Int J Cancer, 2011. **128**(6): p. 1327-34.

72. Brennecke, J., et al., *Principles of MicroRNA–Target Recognition.* PLoS Biology, 2005. **3**(3): p. e85.

73. Brennecke, J., et al., *Principles of microRNA-target recognition.* PLoS biology, 2005. **3**(3): p. e85-e85.

74. Gaul, D.A., et al., *Highly-accurate metabolomic detection of early-stage ovarian cancer.* Scientific Reports, 2015. **5**: p. 16351.

75. Hou, J.M., et al., *Circulating Tumor Cells as a Window on Metastasis Biology in Lung Cancer.* Am J Pathol, 2011. **178**(3): p. 989-96.

76. Young, D.L. and S. Fields, *The role of functional data in interpreting the effects of genetic variation.* Mol Biol Cell, 2015. **26**(22): p. 3904-8.

77. Cenik, C., et al., *Integrative analysis of RNA, translation, and protein levels reveals distinct regulatory variation across humans.* Genome Res, 2015. **25**(11): p. 1610-21.

78. Vignot, S., et al., *Comparative analysis of primary tumour and matched metastases in colorectal cancer patients: evaluation of concordance between genomic and transcriptional profiles.* Eur J Cancer, 2015. **51**(7): p. 791-9.

79. Lili, L.N., et al., *Molecular profiling supports the role of epithelial-to-mesenchymal transition (EMT) in ovarian cancer metastasis.* Journal of Ovarian Research, 2013. **6**(1): p. 49.

80. Jewer, M., S.D. Findlay, and L.M. Postovit, *Post-transcriptional regulation in cancer progression: Microenvironmental control of alternative splicing and translation.* J Cell Commun Signal, 2012. **6**(4): p. 233-48.

81. Truitt, M.L. and D. Ruggero, *New frontiers in translational control of the cancer genome.* Nat Rev Cancer, 2016. **16**(5): p. 288-304.

82. Mertins, P., et al., *Proteogenomics connects somatic mutations to signalling in breast cancer.* Nature, 2016. **534**(7605): p. 55-62.

83. Zhang, B., et al., *Proteogenomic characterization of human colon and rectal cancer.* Nature, 2014. **513**(7518): p. 382-7.

84. Zhang, H., et al., *Integrated Proteogenomic Characterization of Human High-Grade Serous Ovarian Cancer.* Cell, 2016. **166**(3): p. 755-765.

85. Huttlin, E.L., et al., *A tissue-specific atlas of mouse protein phosphorylation and expression.* Cell, 2010. **143**(7): p. 1174-89.

86. Eng, J.K., A.L. McCormack, and J.R. Yates, *An approach to correlate tandem mass spectral data of peptides with amino acid sequences in a protein database.* J Am Soc Mass Spectrom, 1994. **5**(11): p. 976-89.

87. Peng, J., et al., *Evaluation of multidimensional chromatography coupled with tandem mass spectrometry (LC/LC-MS/MS) for large-scale protein analysis: the yeast proteome.* J Proteome Res, 2003. **2**(1): p. 43-50.

88. Elias, J.E. and S.P. Gygi, *Target-decoy search strategy for increased confidence in large-scale protein identifications by mass spectrometry.* Nat Methods, 2007. **4**(3): p. 207-14.

89. Chen, W., J.M. Smeekens, and R. Wu, *Comprehensive analysis of protein N-glycosylation sites by combining chemical deglycosylation with LC-MS.* J Proteome Res, 2014. **13**(3): p. 1466-73.

90. Chen, W., J.M. Smeekens, and R. Wu, *A universal chemical enrichment method for mapping the yeast N-glycoproteome by mass spectrometry (MS).* Mol Cell Proteomics, 2014. **13**(6): p. 1563-72.

91. Wu, R., et al., *A large-scale method to measure absolute protein phosphorylation stoichiometries.* Nat Methods, 2011. **8**(8): p. 677-83.

92. Eng, J.K., A.L. McCormack, and J.R. Yates, *An approach to correlate tandem mass spectral data of peptides with amino acid sequences in a protein database.* Journal of the American Society for Mass Spectrometry, 1994. **5**(11): p. 976-989.

93. Miller, J.A., et al., *Strategies for aggregating gene expression data: the collapseRows R function.* BMC Bioinformatics, 2011. **12**: p. 322.

94. Betel, D., et al., *Comprehensive modeling of microRNA targets predicts functional non-conserved and non-canonical sites.* Genome Biol, 2010. **11**(8): p. R90.

95. Shi, W., et al., *Functional analysis of multiple genomic signatures demonstrates that classification algorithms choose phenotype-related genes.* Pharmacogenomics J, 2010. **10**(4): p. 310-23.

96. Xiao, H. and R. Wu, *Quantitative investigation of human cell surface N-glycoprotein dynamics.* Chemical Science, 2017. **8**(1): p. 268-277.

97. Tian, Q., et al., *Integrated genomic and proteomic analyses of gene expression in Mammalian cells.* Mol Cell Proteomics, 2004. **3**(10): p. 960-9.

98. Lundberg, E., et al., *Defining the transcriptome and proteome in three functionally different human cell lines.* Mol Syst Biol, 2010. **6**: p. 450.

99. Schwanhausser, B., et al., *Global quantification of mammalian gene expression control.* Nature, 2011. **473**(7347): p. 337-42.

100. Heerboth, S., et al., *EMT and tumor metastasis.* Clin Transl Med, 2015. **4**: p. 6.

101. Tsai, J.H. and J. Yang, *Epithelial-mesenchymal plasticity in carcinoma metastasis.* Genes Dev, 2013. **27**(20): p. 2192-206.

102. Maier, T., M. Guell, and L. Serrano, *Correlation of mRNA and protein in complex biological samples.* FEBS Lett, 2009. **583**(24): p. 3966-73.

103. Clarke, C., et al., *Integrated miRNA, mRNA and protein expression analysis reveals the role of post-transcriptional regulation in controlling CHO cell growth rate.* BMC Genomics, 2012. **13**: p. 656.

104. Iwakawa, H.O. and Y. Tomari, *The Functions of MicroRNAs: mRNA Decay and Translational Repression.* Trends Cell Biol, 2015. **25**(11): p. 651-65.

105. Buick, R.N., R. Pullano, and J.M. Trent, *Comparative properties of five human ovarian adenocarcinoma cell lines.* Cancer Res, 1985. **45**(8): p. 3668-76.

106. Jewer, M., S.D. Findlay, and L.M. Postovit, *Post-transcriptional regulation in cancer progression : Microenvironmental control of alternative splicing and translation.* J Cell Commun Signal, 2012. **6**(4): p. 233-48.

107. Meric-Bernstam, F. and G.B. Mills, *Overcoming implementation challenges of personalized cancer therapy.* Nat Rev Clin Oncol, 2012. **9**(9): p. 542-8.

108. Bonora, M., et al., *Molecular mechanisms of cell death: central implication of ATP synthase in mitochondrial permeability transition.* Oncogene, 2015. **34**(12): p. 1608.

109. van Kouwenhove, M., M. Kedde, and R. Agami, *MicroRNA regulation by RNA-binding proteins and its implications for cancer.* Nat Rev Cancer, 2011. **11**(9): p. 644-56.

110. Fang, Z. and N. Rajewsky, *The impact of miRNA target sites in coding sequences and in 3'UTRs.* PLoS One, 2011. **6**(3): p. e18067.

111. Catalanotto, C., C. Cogoni, and G. Zardo, *MicroRNA in Control of Gene Expression: An Overview of Nuclear Functions.* International journal of molecular sciences, 2016. **17**(10): p. 1712.

112. Sohel, M.H., *Extracellular/Circulating MicroRNAs: Release Mechanisms, Functions and Challenges.* Achievements in the Life Sciences, 2016. **10**(2): p. 175-186.

113. Hanahan, D. and Robert A. Weinberg, *Hallmarks of Cancer: The Next Generation.* Cell, 2011. **144**(5): p. 646-674.